Electronic Supplementary Information

Quantitatively differentiating foliar adhesion and absorption of different lead-based particles on *Solanum Melongena* L.

Bing Zhao [ac‡], *Siyu Zhang* [a‡], *Xuejiao Zhang* [a], *Qing Zhao* [*ab], *Jason C. White* [d], *Fengchang Wu* [e], *Baoshan Xing* [f]

[a] Key Laboratory of Pollution Ecology and Environmental Engineering, Institute of Applied Ecology, Chinese Academy of Sciences, Shenyang, 110016, China

[b] National-Regional Joint Engineering Research Center for Soil Pollution Control and Remediation in South China, Guangdong Key Laboratory of Integrated Agro-environmental Pollution Control and Management, Institute of Eco-environmental and Soil Sciences, Guangdong Academy of Sciences, Guangzhou, 510650, China

[c] University of Chinese Academy of Sciences, Beijing, 100049, China

[d] Department of Analytical Chemistry, The Connecticut Agricultural Experiment Station, New Haven, Connecticut 06504, United States

[e] State Key Laboratory of Environmental Criteria and Risk Assessment, Chinese Research Academy of Environmental Sciences, Beijing 100012, China

[f] Stockbridge School of Agriculture, University of Massachusetts, Amherst, MA 01003, USA

*E-mail: zhaoqing@iae.ac.cn

‡ Bing Zhao and Siyu Zhang contributed equally to this paper

List of Supplementary Data

Text S1 Materials

Lead acetate of analytical reagent were obtained from Fu Chen (Tianjin) Chemical Reagent Co., Ltd. Cysteine (99%), thioacetamide (≥ 98.0%), ethanediol (98%) and cetyltrimethylammonium bromine (99%) were from Shanghai Aladdin Biochemical Technology Co., Ltd. Chloroform (≥ 99.0%), EDTA-2Na (≥ 99.9%) was from Shanghai Aladdin Biochemical Technology Co., Ltd. Nitric acid (HNO_3, 69% ~ 70%, trace metal < 1 ppb) of guaranteed reagent grade was obtained from ANPEL Laboratory Technologies (Shanghai) Inc. Perchloric acid ($HClO_4$, 70% ~ 72%) and hydrogen peroxide (H_2O_2, ≥ 30%) of guaranteed reagent grade were obtained from Tianjin Kemiou Chemical Reagent Co., Ltd. Phosphate buffered solution (PBS, 0.1 M) was purchased from Beijing LabLead Biotechnology Co., Ltd. Osmium tetroxide was prepared by Beijing Electron Microscopy China Technology Co., Ltd. Glutaraldehyde fixation solution (2%) were obtained from Beijing Leagene Biotechnology Co., Ltd. Ethanol (99.7%) was from Chengdu Kelong Chemical Co., Ltd. Standard substance citrus (GBW10020) and celery (GBW10048) leaves were purchased from National Sharing Platform for Reference Materials. Ultrapure water (resistivity ≥ 18.2 MΩ*cm) was prepared by Milli-Q Direct 8 (Merck Millipore, Germany).

Text S2 Synthesis of PbS particles

Two hydrophilic-hydrophobic property of lead sulfide nanoparticles (PbS) were prepared in laboratory following previously reported methods.[1,2] Hydrophobic PbS (PbS-S) were prepared by mixing 0.379 g lead acetate, 0.152 g thioacetamide and 0.364 g cetyltrimethylammonium bromine in 40 mL water. The mixture was stirred for 30 min, heated for 14 h at 120 °C, and then cooled to room temperature. Hydrophilic PbS (PbS-Q) were prepared by mixing 0.379 g lead acetate and

0.121 g cysteine in 10 mL ethanediol and 30 mL water. The mixture was stirred for 30 min, heated for 17 h at 150 °C, and cooled to room temperature.

Black solid products were separated by centrifugation at 3500 rpm for 20 min. Precipitates were washed three times with distilled water and ethanol, and then dried at room temperature for 5 h in a vacuum-dryer. Prepared PbS collected in sealed, oxygen-free centrifuge tubes.

Text S3 Preparation of lead-based particles (PbX_n) stock solution

The as-prepared PbS were sonicated at 800 W in a water bath ultrasonicator (KQ-300B, Kunshan, China) for 3 h to obtain 1000 mg Pb L^{-1} evenly dispersed suspension. Bulk Pb oxides were ground into large sheets to facilitate dispersing, and then sonicated at 720 W with an immersing probe in ultrasonic cell disrupter (1800-99, Biosafer, China) for 3 h to obtain 2000 mg Pb L^{-1} suspension.

Two dissolvable Pb salts ($PbSO_4$ and $PbCl_2$) were used for comparison with the particles. The salts were dissolved in distilled water directly with assistance of ultrasonication to obtain 100 mg Pb L^{-1} solution. Before the plant experiment, the PbX_n suspension/solution was kept sealed and stored at 4 °C.

Text S4 Analytical conditions and quality control of inductively coupled plasma-mass spectrometry (ICP-MS)

Working conditions: sampling depth: 3.61 mm; cooling gas flow: 13.0 L min^{-1}; auxiliary gas flow: 0.60 L min^{-1}; atomization gas flow: 0.92 L min^{-1}; analysis pressure: 2.6×10^{-6} mbar; diffusion pressure: 1.8 mbar; atomization pressure: 2.68 bar; power: 1390 W; reflected power: 0.0 W; data

acquisition method: scanning. Analysis time for each sample: 90 s. The detection limit was 0.1 μg L^{-1}, and the quantitation limit was 1 μg L^{-1}.

Before testing the sample, the ICP-MS was calibrated with the calibration solution. A series of Pb standard gradient dilution solutions are introduced into the instrument to form a linear relationship (r > 0.9999). Pb Standard samples were repeatedly measured every 20 experimental samples for calibration, and error values were within ± 10%. Relative standard deviation (RSD) of sample concentration was < 20 %. Reagent and plant blank controls amended with distilled water were analyzed each time with the samples. Recoveries of the digestion and analytical procedures were evaluated by treating standard reference leaves (citrus and celery) following the same procedure.

Text S5 X-ray photoelectron spectroscopy (XPS) analytic conditions

An appropriate amount of sample was pressed onto a sample plate, and the sample was placed in the sample chamber of Thermo Scientific K-Alpha XPS instrument. When the pressure of the sample chamber was less than 2.0×10^{-7} mbar, the sample was sent to the analysis chamber. The spot size was 400 μm, the operating voltage was 12 kV, and the filament current was 6 mA. The full scan energy is 150 eV and the step length is 1 eV. The narrow-spectrum scan has a pass energy of 50 eV and a step length of 0.1 eV. Default orbit tests the fine spectra of C, O, Pb, and S elements. The binding energy with surface contamination C1s (284.8 eV) was used as the standard.

Text S6 Fourier transform infrared spectroscopy (FTIR) analytic conditions

In a dry environment, a predetermined amount of sample and an appropriate amount of dry potassium bromide powder were added to the mortar, fully ground multiple times, and then placed on a tablet press (pressed into a transparent sheet). The background is first collected during the test, and then the infrared spectrum of the sample is collected. The resolution is 4 cm^{-1}, the number of scans is 32, and the test wave number range is 400-4000 cm^{-1}.

Text S7 Plant cultivation

A local cultivar of eggplant (*Solanum melongena* L.) was selected in the foliar application experiments. Seeds were cultivated in plastic pots (diameter: 10 cm; height: 9 cm) filled with nutrient substrates (pH: 6.5 ~ 6.8; N, P, K ≥ 12 g kg^{-1}; organic matter contents ≥ 40%; Si ≥ 0.3 g/kg). In each pot, 3 seeds were cultivated at initial, and two of them were removed after germination. All plants were placed in growth chambers (day/night period: 16 h/8 h; temperature: 25 ℃/22 ℃; humidity: 45%/65%) with a photosynthetic luminous power density of 14.5 W m^{-2} in day time period. Plants were watered with tap water (Pb < 0.1 μg L^{-1}) every 2 days to keep humidity of the nutrient substrates at 40%.

Text S8 Scanning electron microscope-energy dispersive spectroscopy (SEM-EDS) sample preparation

Firstly, four leaves of the same age were selected and treated separately, including not treated, washed with deionized water, washed with 20 mM EDTA-2Na solution, and extracted with chloroform. The leaves were cut into small pieces (~ 4 × 4 mm^2), and then immersed in 2% glutaraldehyde for 2 h, washed three times with 0.1 M PBS, and post-fixed with 1% osmium tetroxide in 0.1 M PBS for 1 h at 4 ℃. The specimens were rinsed with PBS and dehydrated in

sequential-graded concentrations of ethanol (30%, 50%, 70%, 80%, 90%, and 100%). Dehydrated samples were freeze dried, and sprayed with gold-palladium by sputter coater (SD-900C, Vision Precision Instruments, China). Structure and surface characteristics of leaves were examined using SEM-EDS operating at an accelerating voltage of 3 kV under ultra-high vacuum conditions (9.6×10^{-5} Pa) and in secondary electron mode.

Text S9 Transmission electron microscopy-energy dispersive spectroscopy (TEM-EDS) sample preparation

Plant leaves cut into small pieces (1 ~ 2 mm in length). To determine Pb localization within plant leaves, plant samples were fixed in 3% glutaraldehyde in 0.2 M phosphate buffer (pH 7.2) at 4 ˚C overnight, washed 3 times with 0.1 M phosphate buffer (pH 7.2), and post-fixed with 1% osmium tetroxide in 0.1 M phosphate buffer (pH 7.2) for 1 h at 4 ˚C. They were then dehydrated in a graded series of ethanol (50%, 70%, 80%, 90%, 95% and 100%), 15 min for each step. The dehydrated samples were finally embedded in 100% Spurr resin (Spurr, 1969) and sectioned (90 nm thickness) for TEM (JEOL JEM-2100, Japan) at an accelerating voltage of 200 kV. Elemental composition in the selected areas was determined by EDS coupled to the JEM-2100 (JEOL, Japan).

Text S10 Robustness evaluation of equation

The robustness of Eqs. (3) ~ (6) was evaluated through an initial two step development: (1) splitting the data into training and validation sets validating the data via internal and external certification. To split the data into training and validation sets, we first sorted the 25 data based on decreasing maximum *Ad*, *Ab*, *CAb* and *SAb* value. Second, the data were split into three sets: the lowest *Ad*, *Ab*, *CAb* and *SAb* value were grouped into the validation set V_2 to represent the data

that are not within the range of the training set. The remaining 23 data molecules were split into two sets: training set (T) and the validation set (V_1) following pattern T-T-T-T-T-T-T-V_1-T-T-T-T-T-T-T-V_1-T-T-T-T-T-T-T to ensure the V_1 set is evenly distributed in the training set.

Text S11 X-ray photoelectron spectroscopy (XPS) analysis

XPS survey spectra of PbX_n showed that the four elemental orbitals of the particle surface were C 1s, O 1s, Pb 4f and S 2p, respectively (Fig. S4). The C 1s spectrum of PbX_n was fitted with two peaks after charge calibration (Fig. S5): the first peak at 284.8 eV was attributed to C-C; the second peak of PbS at 287.2 eV ascribed to C-O single bonds; and the second peak of Pb_3O_4, PbO_2 and PbO at 288.9 ~ 289.0 eV to O=C-O.[3-6] The first peak and the second peak of PbS were likely the result of adventitious carbon contamination or the background of the XPS test,[7,8] while the second peak of Pb_3O_4, PbO_2 and PbO was due to carbonate ions.[9] Carbonate fromed from the reaction of oxidized lead with atmospheric CO_2.[10] As shown in Fig. S6, the decomposed O 1s XPS spectra of PbX_n presents as three distinct varieties of oxygen, involving metal oxides (528.9 ~ 530.0 eV), hydroxyl bond (531.0 ~ 531.7 eV) and adsorbed water/hydroxides (532.2 eV).[11-13] For the two PbS (Fig. S7), S 2p peaks having a spin-orbit doublet consisting of S $2p_{3/2}$ and S $2p_{1/2}$ (Δ = 1.2 or 1.3 eV). In this regard, the S $2p_{3/2}$ peaks at 160.7 eV and 160.6 eV can be assigned to sulfide in galena, which agrees well with literature (160.80 and 160.70 eV).[14,15] The Pb 4f spectra of PbX_n consists of spin-orbit splitting into Pb $4f_{7/2}$ and Pb $4f_{5/2}$ components (Fig. S8). The Pb $4f_{7/2}$ peaks at 137.2 ~ 138.9 eV could be attributed to lead sulfides (Pb-S) or Pb-O-containing species (Fig. S8).[13,16-18] Previous studies have shown that the binding energies of Pb oxides/hydroxides (*e.g.* PbO, PbO_2, and $Pb(OH)_2$) and PbS are almost the same.[19]

Text S12. Fourier transform infrared spectroscopy (FTIR) analysis

As shown in Fig. S9, the frequencies due to the molecules of PbS were confirmed by the peaks at 700 ~ 600 and 1100 ~ 1000 cm^{-1}.[20,21] The oxidized lead characteristic peaks at 460 ~ 400 cm^{-1} and 550 ~510 cm^{-1}, assigned to the vibration modes of Pb-O bond.[22,23] The response at 1000 ~ 800 cm^{-1} may also be the characteristic peak of Pb.[21,24] The peak at ~1527 cm^{-1} was attributed to lead compounds or Pb^{2+}.[25,26] 1500 ~ 1300 cm^{-1} was the in-plane bending vibration peaks of δ(O-H).[27] 1300 ~ 900 and 900 ~ 500 cm^{-1} were the stretching vibration peak of ν[C-O(H)] and the out-of-plane bending vibration peaks of γ(C-H), respectively.[26,28] δ(O-H) in the five lead species comes from hydroxide in water, while ν[C-O(H)] and γ(C-H) in PbS-Q and PbS-S are related to particle synthesis process.

Text S13 Raman spectroscopy analysis

As shown in Fig. S10, the Raman peaks occurred at 78 ~ 81 cm^{-1} and 135 ~ 144 cm^{-1} correspond to a combination of longitudinal and transverse acoustic modes, which are typical peaks of inorganic lead compounds.[29,30] Peak observed at 966 and 969 cm^{-1} may be due to laser-induced degradation of PbS.[31,32] Pawar *et al.*[30] discovered 131, 426 and 962 cm^{-1} as typical peaks for PbS nanostars. The characteristic peaks that correspond to the Pb_3O_4 appear at 542 cm^{-1}, and were attributed to the symmetric bending vibrational modes of Pb (II, IV)-O bonds.[33-35] Oxidized lead characteristic peaks at ~270, 319 and 335 cm^{-1}, assigned to the vibration modes of Pb-O bond, were matched well with the Raman standard peaks.[22,23,36]

Table S1 BET surface area of PbX_n

Treatment	BET surface area/m^2 g^{-1}
PbS-S	3.1
PbS-Q	7.6
Pb_3O_4	5.8
PbO_2	0.8
PbO	5.7

Table S2 Removal efficiency (%) of Pb species on eggplant leaves by deionized water

Day	PbS-S	PbS-Q	Pb_3O_4	PbO_2	PbO	$PbSO_4$	$PbCl_2$
2^{nd}	15	27	13	12	30	17	38
4^{th}	9	25	15	14	17	13	28
6^{th}	10	13	14	11	16	11	14
8^{th}	4	6	18	21	16	11	16
11^{th}	6	7	7	9	11	11	15
15^{th}	5	7	10	10	10	11	16
22^{nd}	4	6	9	6	4	8	18

Table S3 Percentages (%) of Pb species absorbed by eggplant leaves

Days	PbS-S	PbS-Q	Pb_3O_4	PbO_2	PbO	$PbSO_4$	$PbCl_2$
2^{nd}	57	34	23	6	4	0.4	4
4^{th}	59	40	20	7	5	2	4
6^{th}	59	31	16	14	5	4	8
8^{th}	57	35	15	12	10	3	7
11^{th}	59	36	12	13	9	3	6
15^{th}	60	34	13	15	9	3	8
22^{nd}	64	34	14	15	9	4	9

Table S4 Percentages (%) of Pb species adhered to eggplant leaves

Days	PbS-S	PbS-Q	Pb_3O_4	PbO_2	PbO	$PbSO_4$	$PbCl_2$
2nd	29	39	63	82	66	82	59
4th	32	35	65	80	79	85	68
6th	32	56	70	75	79	85	78
8th	39	58	67	67	74	86	77
11th	35	57	81	78	80	86	79
15th	35	58	77	75	81	86	76
22nd	32	60	77	78	88	87	73

Table S5 Percentages ($M_{Adhesion}/M_{Uptake}$, %) of Pb species adhered to eggplant leaves

Days	PbS-S	PbS-Q	Pb_3O_4	PbO_2	PbO	$PbSO_4$	$PbCl_2$
2nd	33	52	72	92	93	98	92
4th	35	47	76	92	94	97	94
6th	35	64	81	84	93	95	91
8th	40	62	82	84	87	96	91
11th	37	61	87	86	89	96	92
15th	37	63	85	83	90	96	90
22nd	33	63	84	83	91	95	89

Table S6 Percentages ($M_{ABA}/M_{Absorption}$, %) of Pb species absorbed via the cuticle pathway by eggplant leaves

Days	PbS-S	PbS-Q	Pb_3O_4	PbO_2	PbO	$PbSO_4$	$PbCl_2$
2nd	43	48	46	36	43	127	80
4th	41	45	51	30	31	119	73
6th	37	69	57	19	37	101	50

Table S7 Analysis of variance of multi linear regression

		Sum of Squares	df	Mean Square	F	Sig.
Ad	Regression	6654.507	4	1663.627	425.083	0.000
	Residual	78.273	20	3.914		
	Total	6732.780	24			
Ab	Regression	8942.801	4	2235.700	411.095	0.000
	Residual	108.768	20	5.438		
	Total	9051.569	24			
CAb	Regression	7514.243	3	2504.748	69.509	0.000
	Residual	756.737	21	36.035		
	Total	8270.980	24			
SAb	Regression	7514.243	3	2504.748	69.509	0.000
	Residual	756.737	21	36.035		
	Total	8270.980	24			

Table S8 Pearson correlation between PbX_n properties

	log *L*	log *H*	log *Z*	log *C*	log *B*	log *K*
log *L*	1					
log *H*	0.953**	1				
log *Z*	0.821**	0.785**	1			
log *C*	-0.385	-0.500*	-0.129	1		
log *B*	0.124	0.248	-0.327	-0.841**	1	
log *K*	-0.285	-0.018	-0.488*	-0.471*	0.711**	1

** Significant correlation at 0.01 level (bilateral)
* Significant correlation at 0.05 level (bilateral)

Table S9 Direct and indirect effect of PbX_n properties on adhesion rate via path analysis

Variables	Direct	Indirect				Total
		log *Z*	log *C*	log *K*	log *H*	
log *Z*	0.940	—	0.080	0.164	-0.299	0.885
log *C*	-0.623	-0.121	—	0.159	0.191	-0.394
log *K*	-0.337	-0.459	0.293	—	0.007	-0.496
log *H*	-0.381	0.738	0.312	0.006	—	0.675

Table S10 Direct and indirect effect of PbX_n properties on absorption rate via path analysis

Variables	Direct	Indirect				Total
		log *Z*	log *C*	log *K*	log *H*	
log *Z*	-0.832	—	-0.091	-0.184	0.253	-0.854
log *C*	0.703	0.107	—	-0.178	-0.161	0.471
log *K*	0.377	0.406	-0.331	—	-0.006	0.446
log *H*	0.322	-0.653	-0.352	-0.007	—	-0.690

Table S11 Direct and indirect effect of PbX_n properties on cuticular absorption rate via path analysis

Variables	Direct	Indirect			Total
		log *B*	log *L*	log *Z*	
log *B*	1.261	—	-0.146	-0.304	0.811
log *L*	-1.175	0.156	—	0.764	-0.255
log *Z*	0.930	-0.412	-0.965	—	-0.447

Table S12 Direct and indirect effect of PbX_n properties on stomatal absorption rate via path analysis

Variables	Direct	Indirect			Total
		log *B*	log *L*	log *Z*	
log *B*	-1.261	—	0.146	0.304	-0.811
log *L*	1.175	-0.156	—	-0.764	0.255
log *Z*	-0.930	0.412	0.965	—	0.447

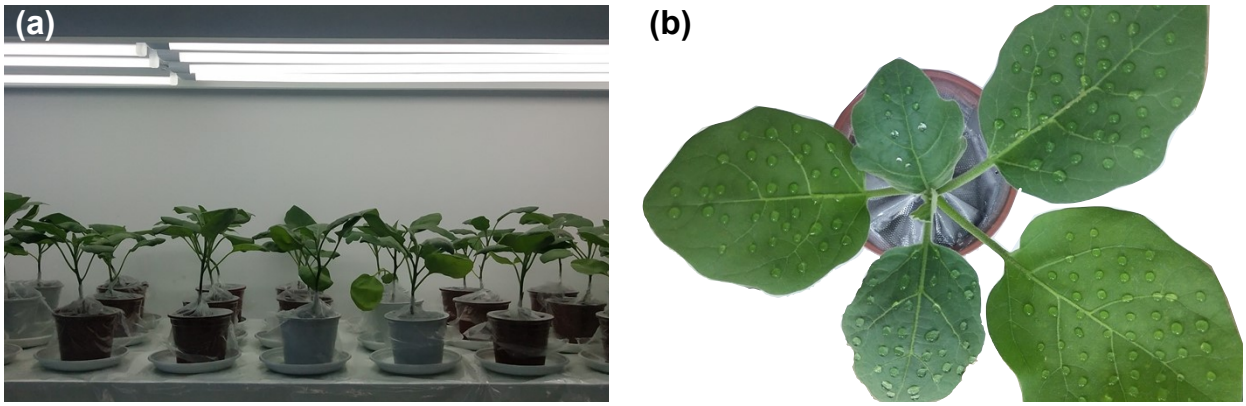

Fig. S1 Photographs of the plants (a) and eggplant leaves after foliar application of 10 mg Pb L^{-1} dispersion (b).

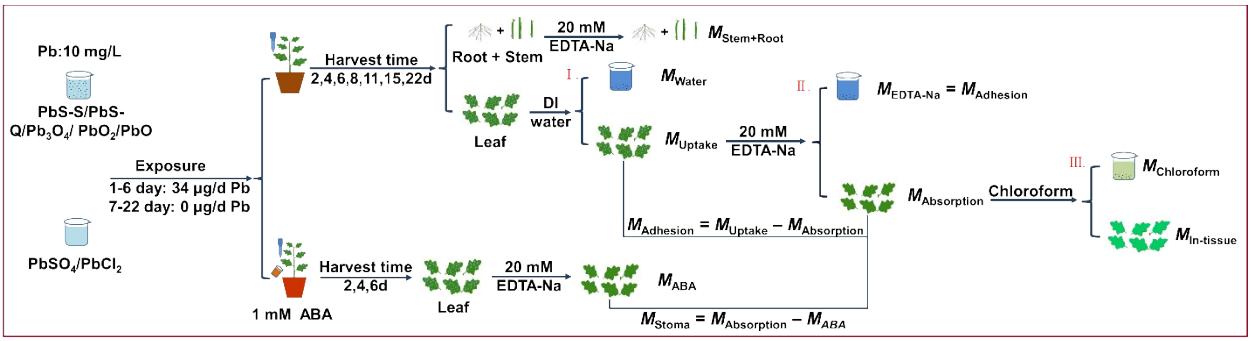

Fig. S2 Schematic illustration of different treatments in the plant Pb exposure experiments. M_{Uptake}: Mass of Pb in leaves after washing with deionized water; M_{Water}: Mass of Pb in deionized water after leaf washing; $M_{Absorption}$: Mass of Pb in leaves after washing with 20 mM EDTA-2Na solution; $M_{Adhesion} = M_{EDTA\text{-}2Na}$: Mass of Pb in EDTA-2Na solution after leaf washing; $M_{Stem+Root}$: Mass of Pb in stems and roots; $M_{Chloroform}$: Mass of Pb in chloroform after leaf washing; $M_{In\text{-}tissue}$: Mass of Pb in leaves after chloroform washing; M_{ABA}: Absorption mass of Pb in leaves after 1 mM ABA was applied to the root of eggplant, that is, the mass of Pb absorbed by leaves through wax; M_{Stoma}: The leaves absorb the mass of Pb through stomata.

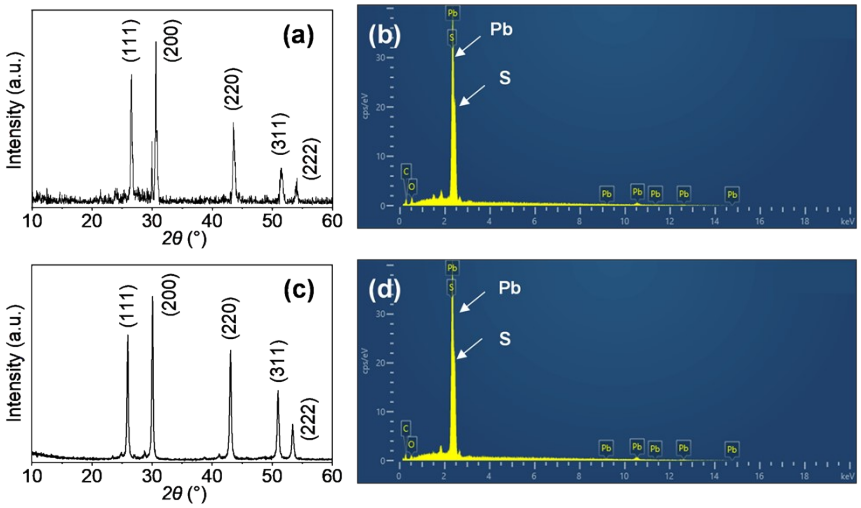

Fig. S3 XRD spectrum (a) and EDS image (b) of as-prepared PbS-S; XRD spectrum (c) and EDS image (d) of as-prepared PbS-Q.

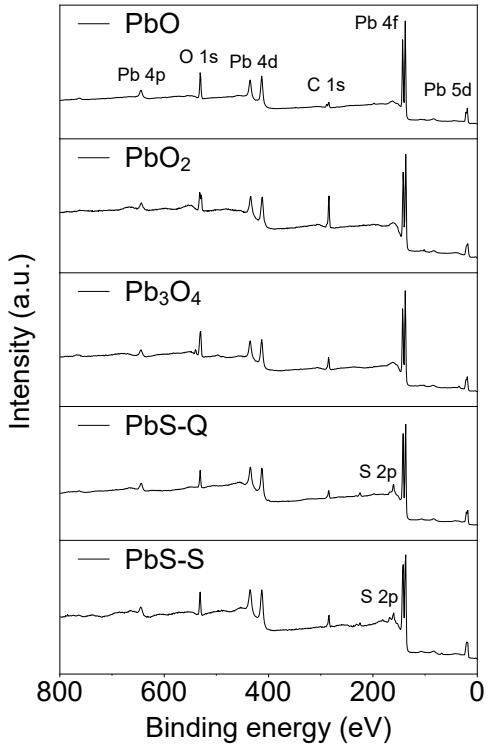

Fig. S4 XPS survey spectra of PbX_n.

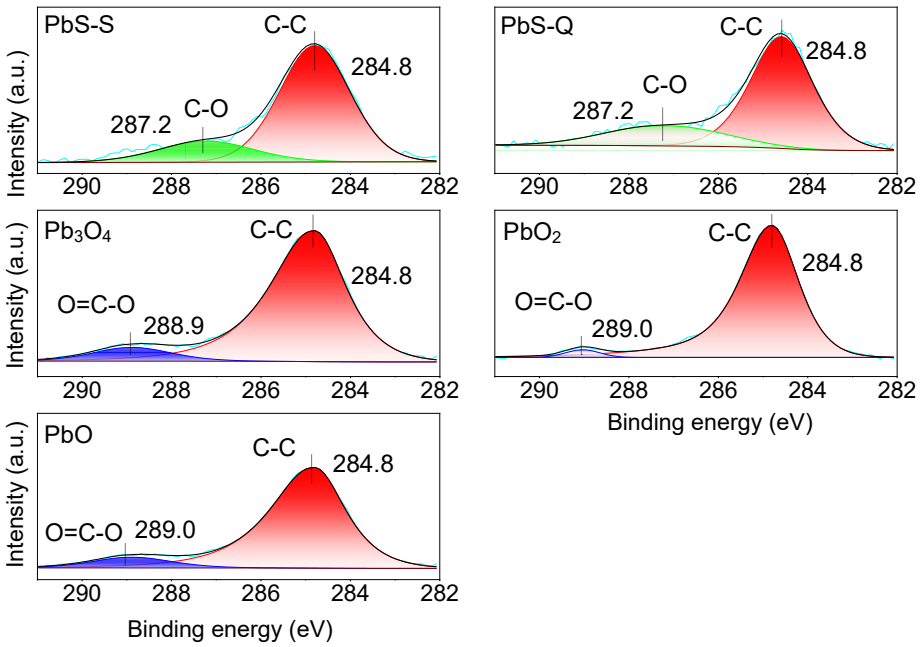

Fig. S5 Fitting results of C 1s spectra of PbX_n.

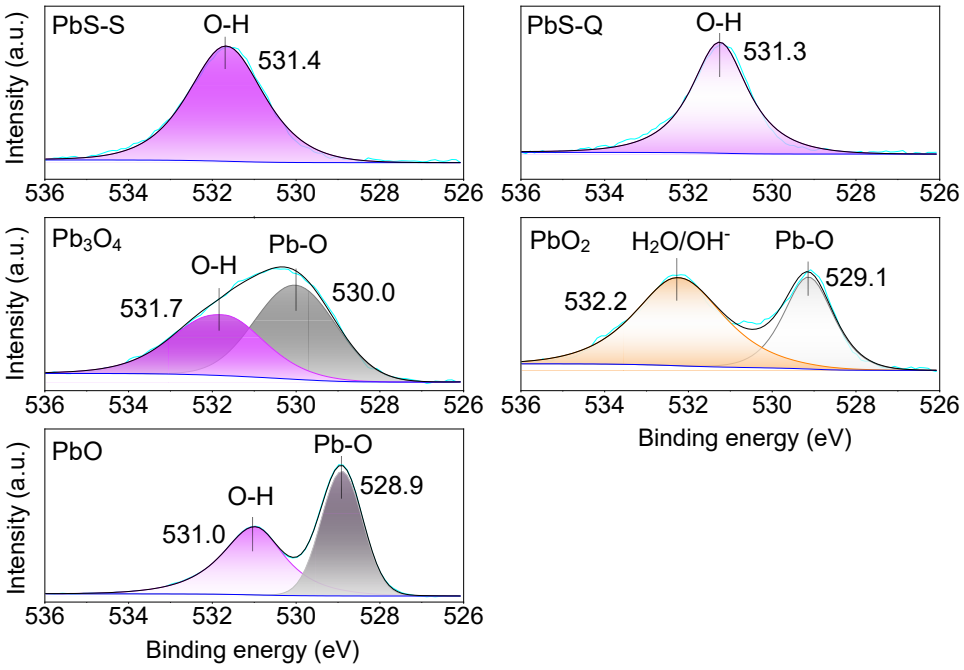

Fig. S6 Fitting results of O 1s spectra PbX_n.

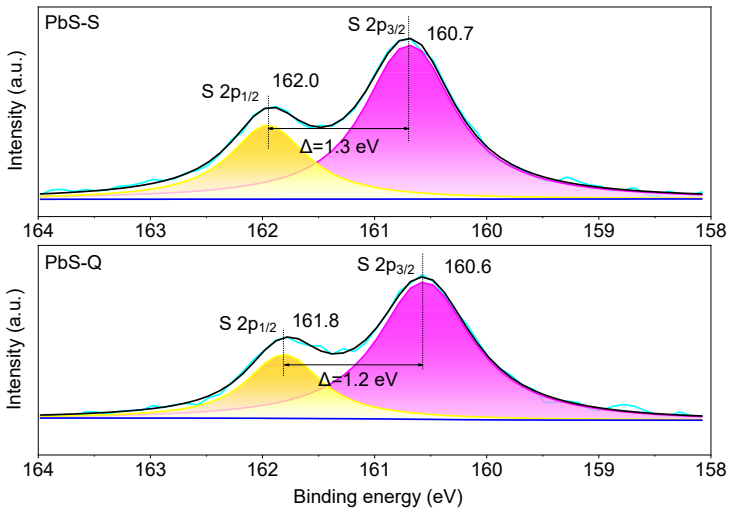

Fig. S7 Fitting results of S 2p spectra of PbX_n.

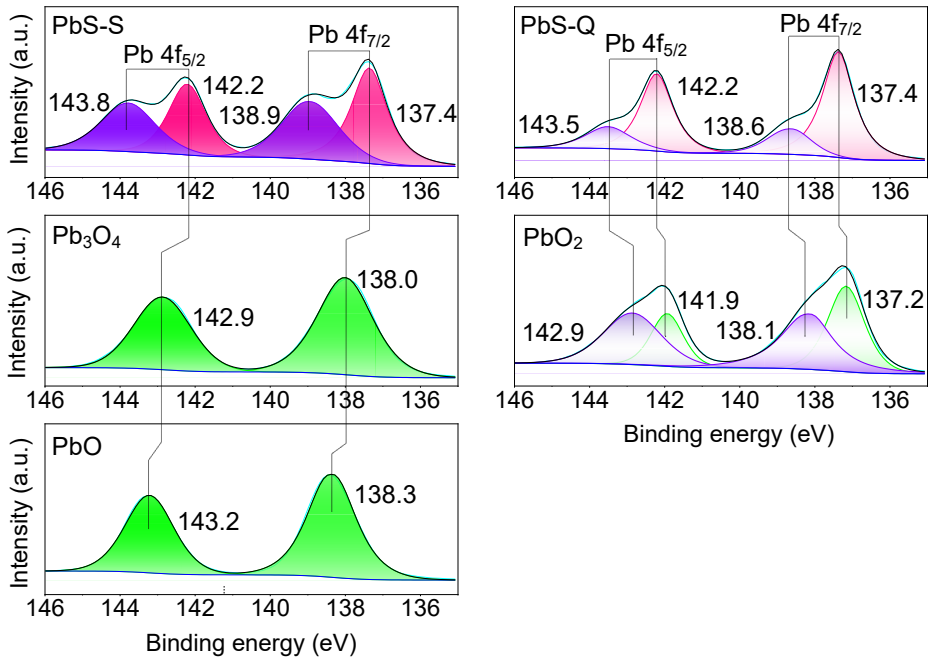

Fig. S8 Fitting results of Pb 4f spectra of PbX_n.

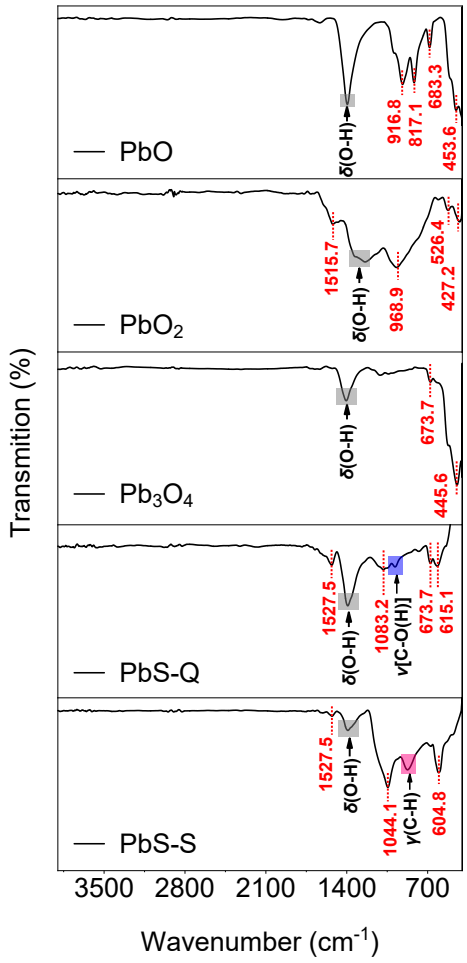

Fig. S9 FT-IR spectra of PbX_n.

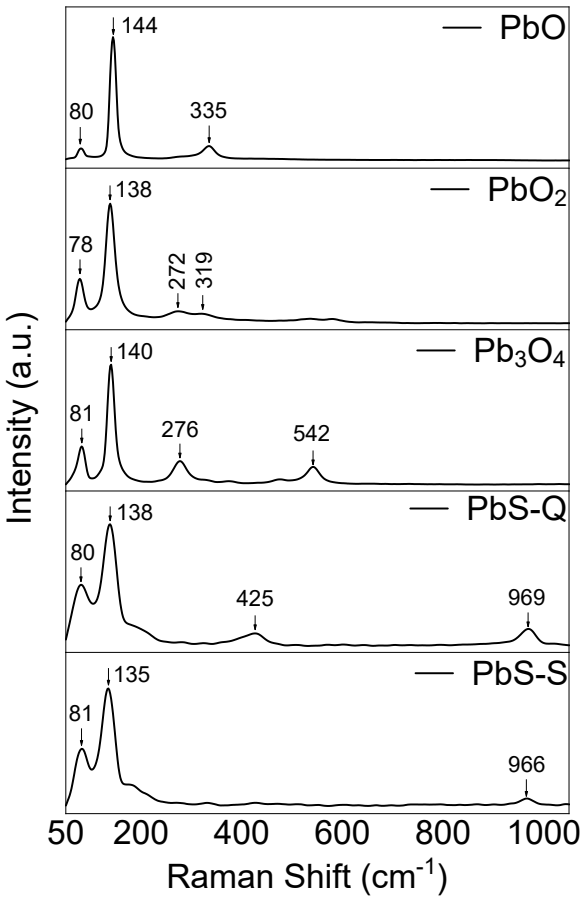

Fig. S10 Raman spectra of PbX_n.

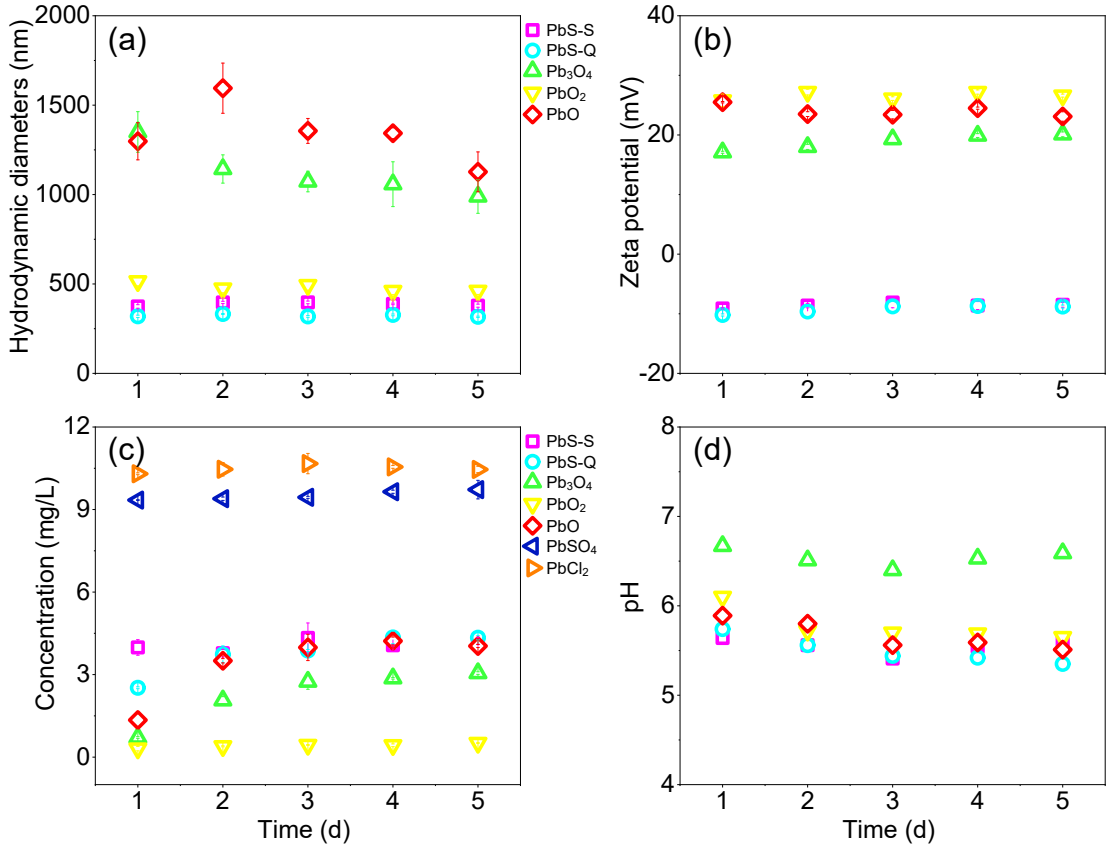

Fig. S11 Characterization of 10 mg Pb L^{-1} PbX_n suspensions and salt solutions. (a) Hydrodynamic diameters; (b) Zeta potential values; (c) Concentrations of Pb ions; (d) pH.

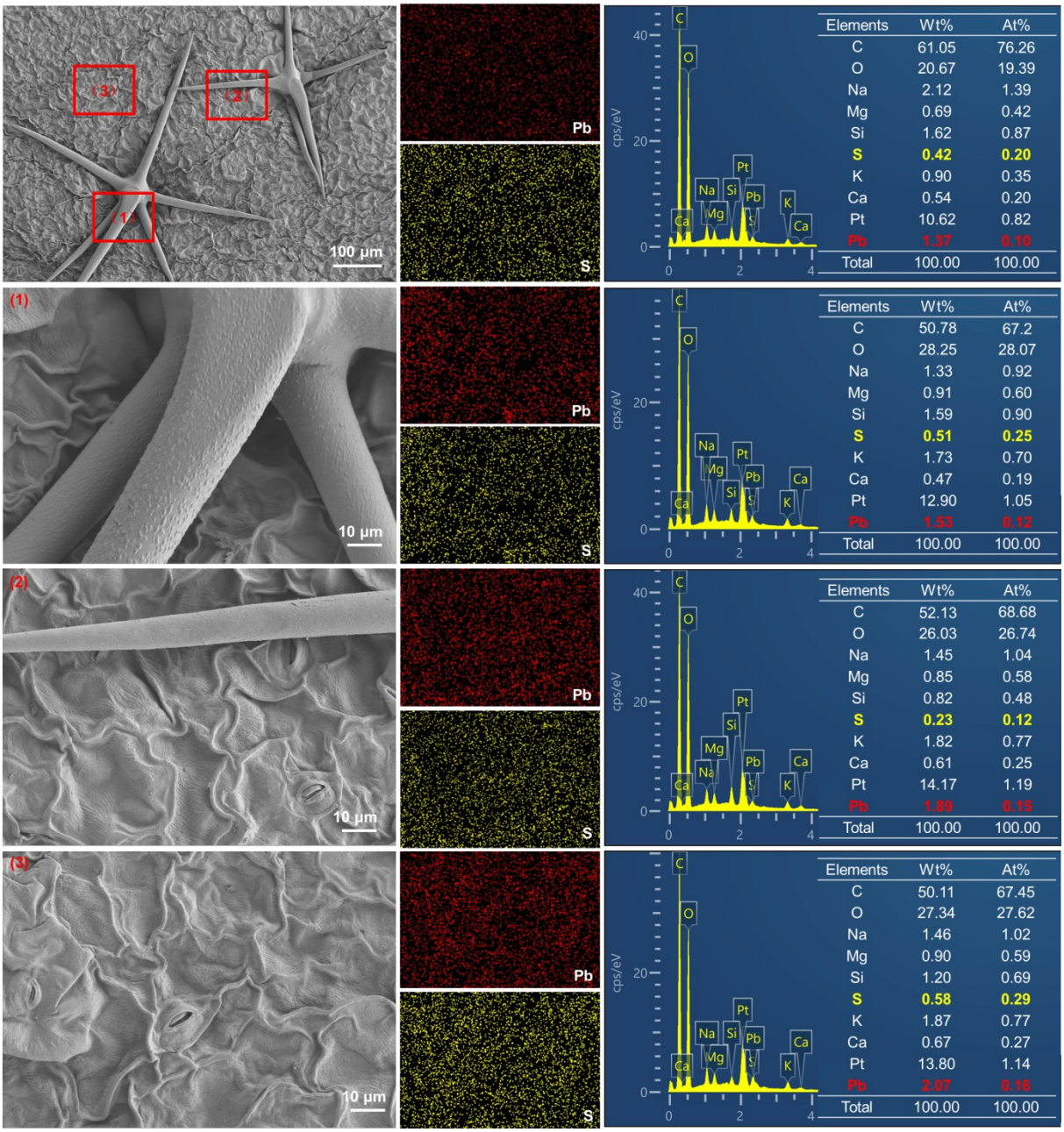

Fig. S12 SEM images of no rinsed eggplant leaves and EDS mapping diagrams of Pb and S elements after exposure to PbS-S (M_{Pb} = 170 μg) for 5 days. Wt%: weight percentage; At%: atomic percentage.

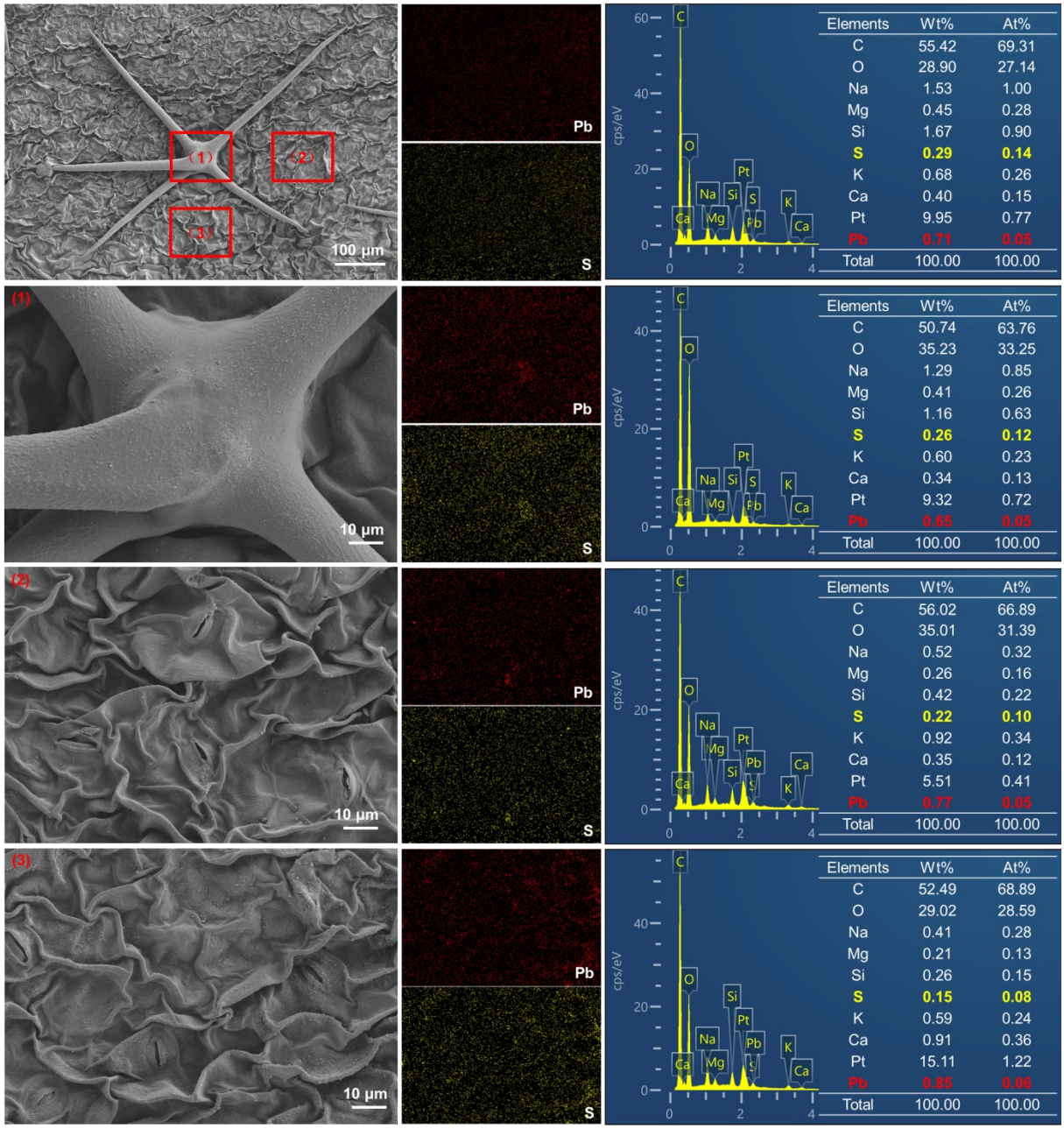

Fig. S13 SEM images and EDS mapping diagrams of Pb and S elements of eggplant leaves rinsed with deionized water after exposure to PbS-S (M_{Pb} = 170 μg) for 5 days. Wt%: weight percentage; At%: atomic percentage.

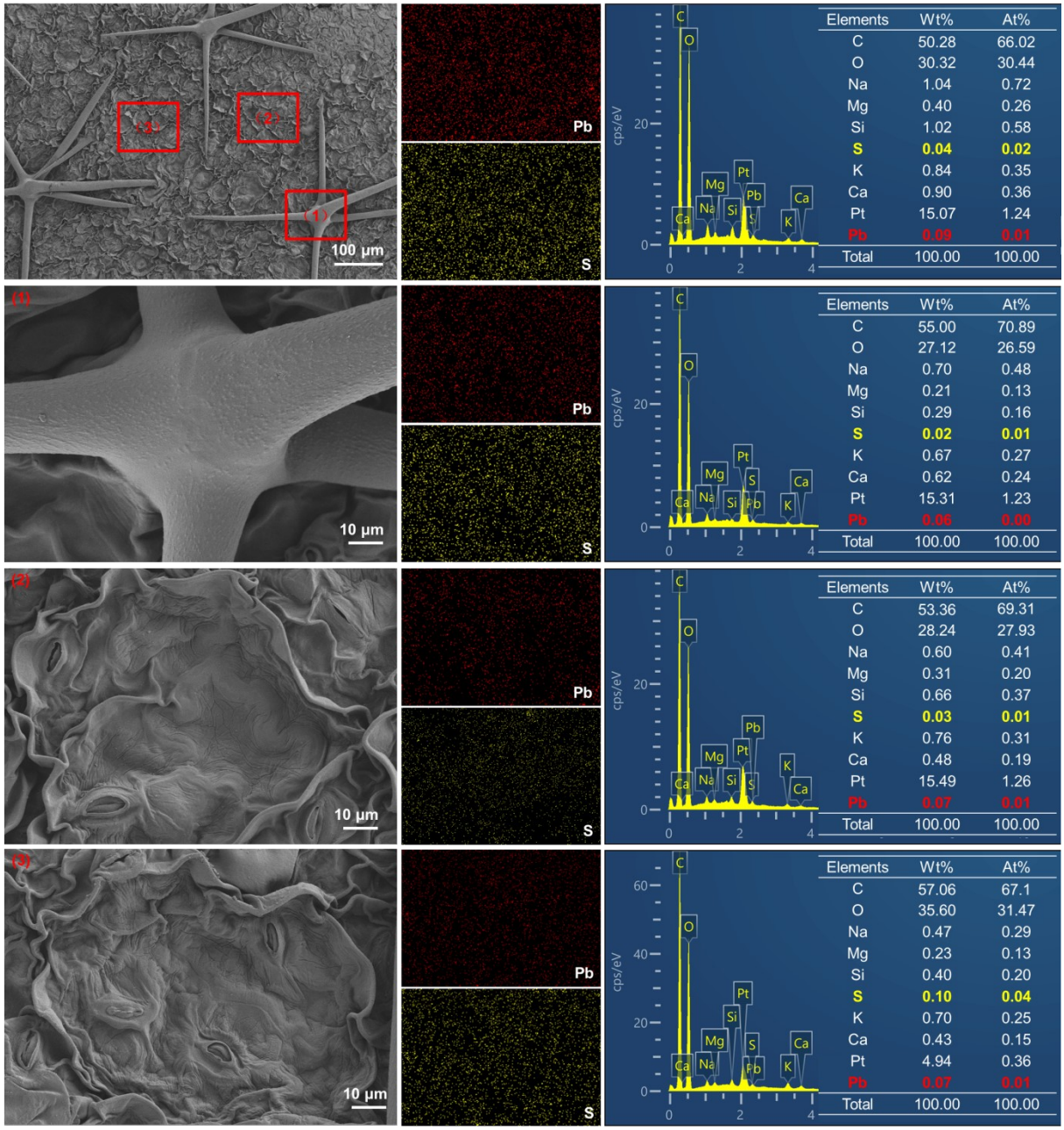

Fig. S14 SEM images and EDS mapping diagrams of Pb and S elements of eggplant leaves rinsed with 20 mM EDTA-2Na solution after exposure to PbS-S (M_{Pb} = 170 μg) for 5 days. Wt%: weight percentage; At%: atomic percentage.

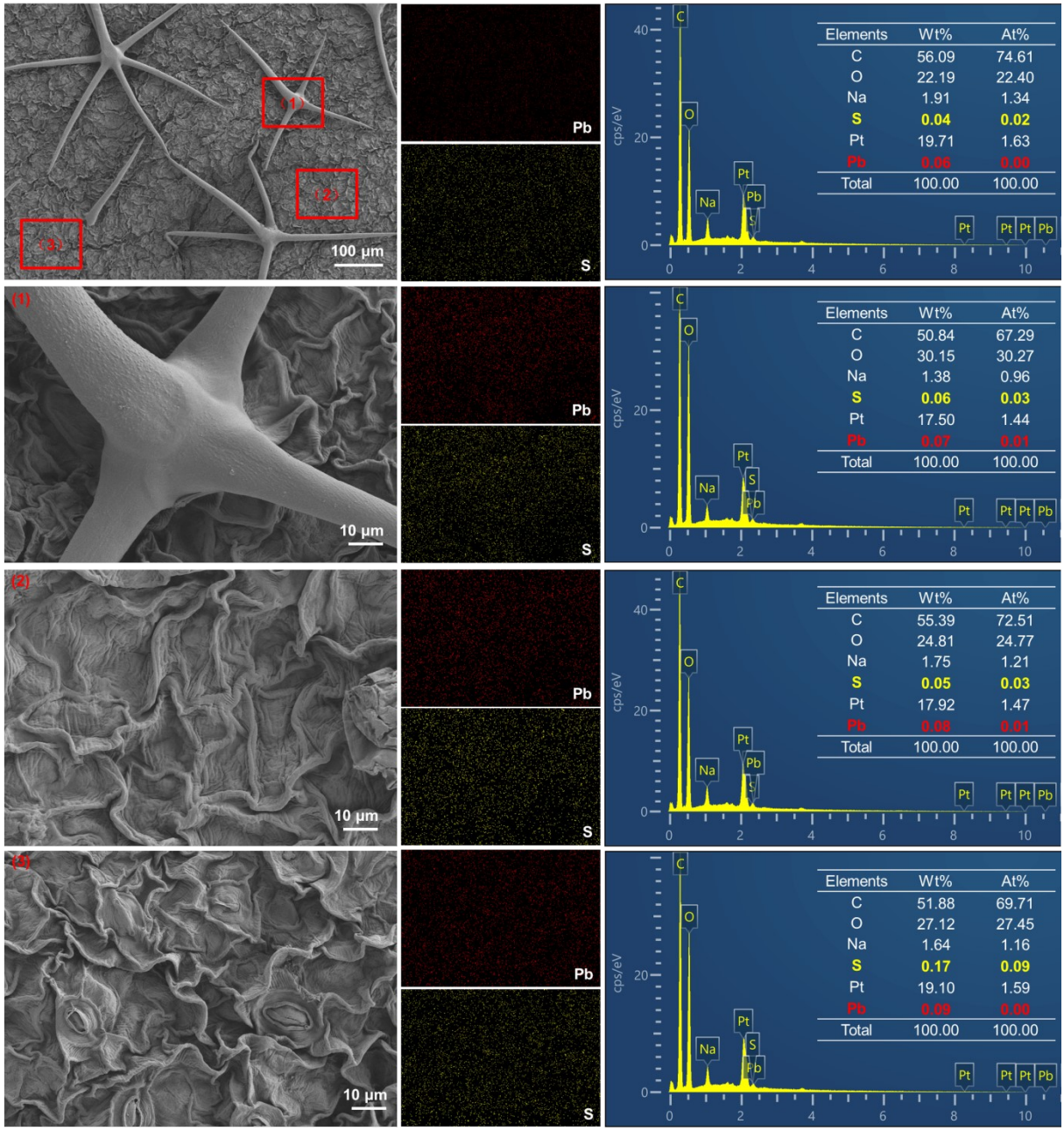

Fig. S15 SEM images and EDS mapping diagrams of Pb and S elements of eggplant leaves rinsed with chloroform after exposure to PbS-S (M_{Pb} = 170 μg) for 5 days. Wt%: weight percentage; At%: atomic percentage.

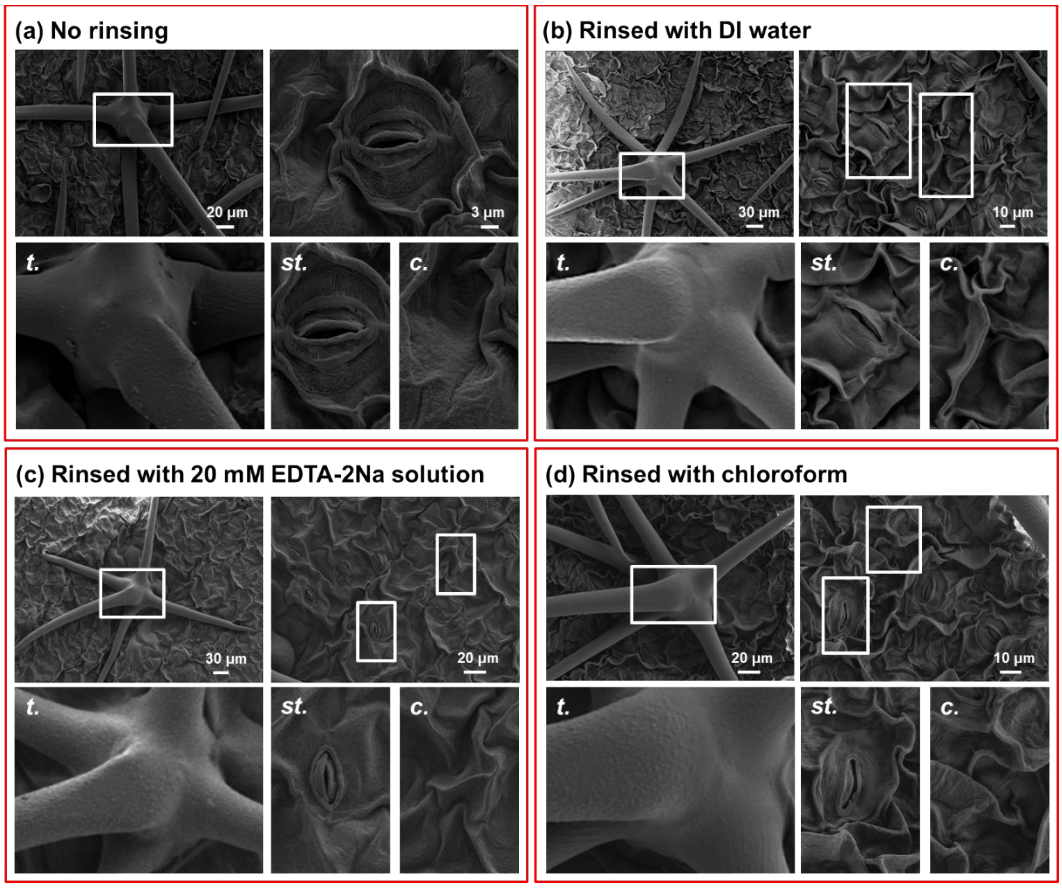

Fig. S16 SEM-EDS images of eggplant leaves after exposure to deionized water for 5 days. (a) No rinsing; (b) Rinsed with deionized water; (c) Rinsed with 20 mM EDTA-2Na solution; (d) Rinsed with chloroform. Enlarged pictures of leaf structures in white boxes are shown in lower panels. *t.*: *trichome*; *st.*: *stoma*; *c.*: *cuticle*.

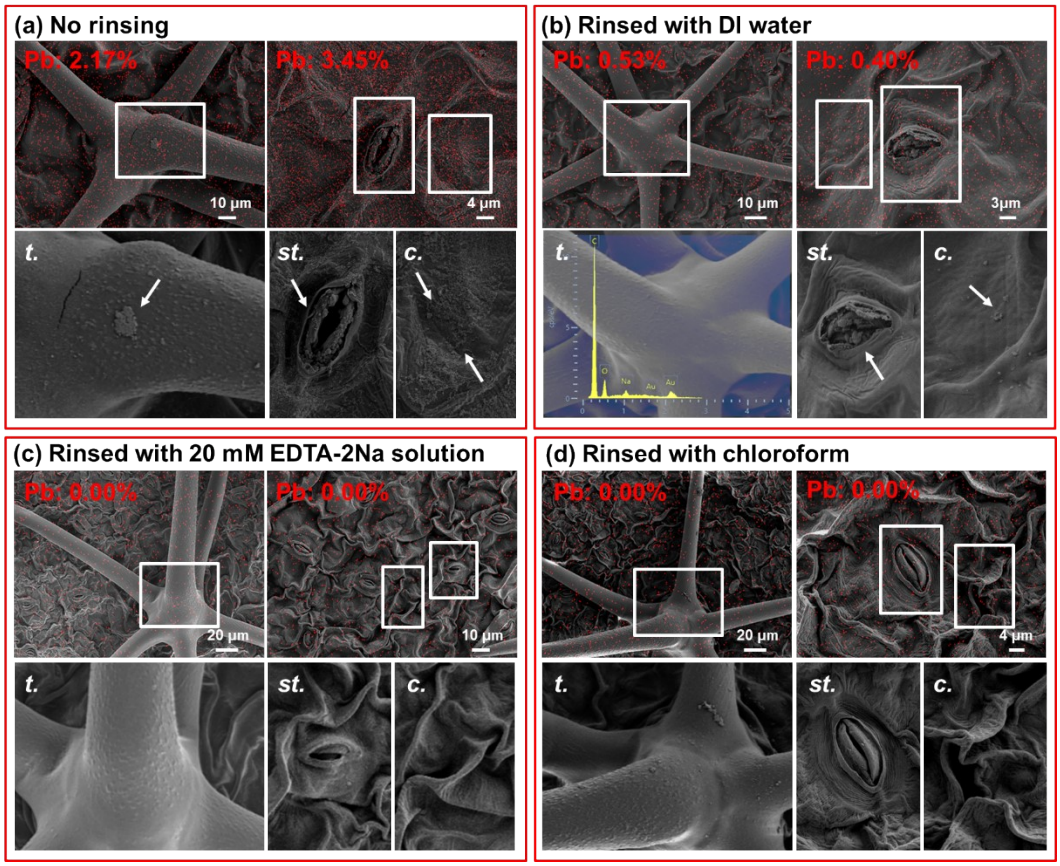

Fig. S17 SEM-EDS images of eggplant leaves after exposure to PbS-Q (M_{Pb} = 170 μg) for 5 days. (a) No rinsing; (b) Rinsed with deionized water; (c) Rinsed with 20 mM EDTA-2Na solution; (d) Rinsed with chloroform. Red dots represent element Pb. Red numbers in upper panels are percentage of element Pb by weight. White arrows indicate large aggregates of PbX_n. Enlarged pictures of leaf structures in white boxes are shown in lower panels. *t.*: *trichome*; *st.*: *stoma*; *c.*: *cuticle*.

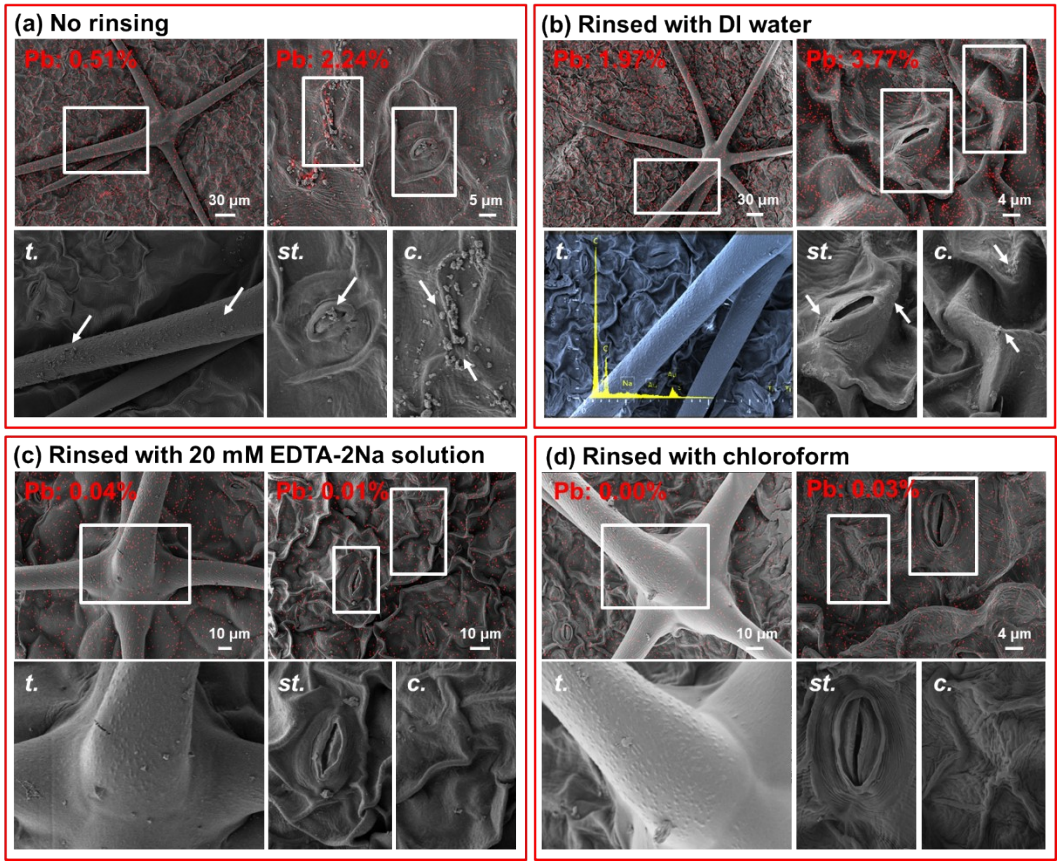

Fig. S18 SEM-EDS images of eggplant leaves after exposure to Pb_3O_4 (M_{Pb} = 170 μg) for 5 days. (a) No rinsing; (b) Rinsed with deionized water; (c) Rinsed with 20 mM EDTA-2Na solution; (d) Rinsed with chloroform. Red dots represent element Pb. Red numbers in upper panels are percentage of element Pb by weight. White arrows indicate large aggregates of PbX_n. Enlarged pictures of leaf structures in white boxes are shown in lower panels. *t.*: *trichome*; *st.*: *stoma*; *c.*: *cuticle*.

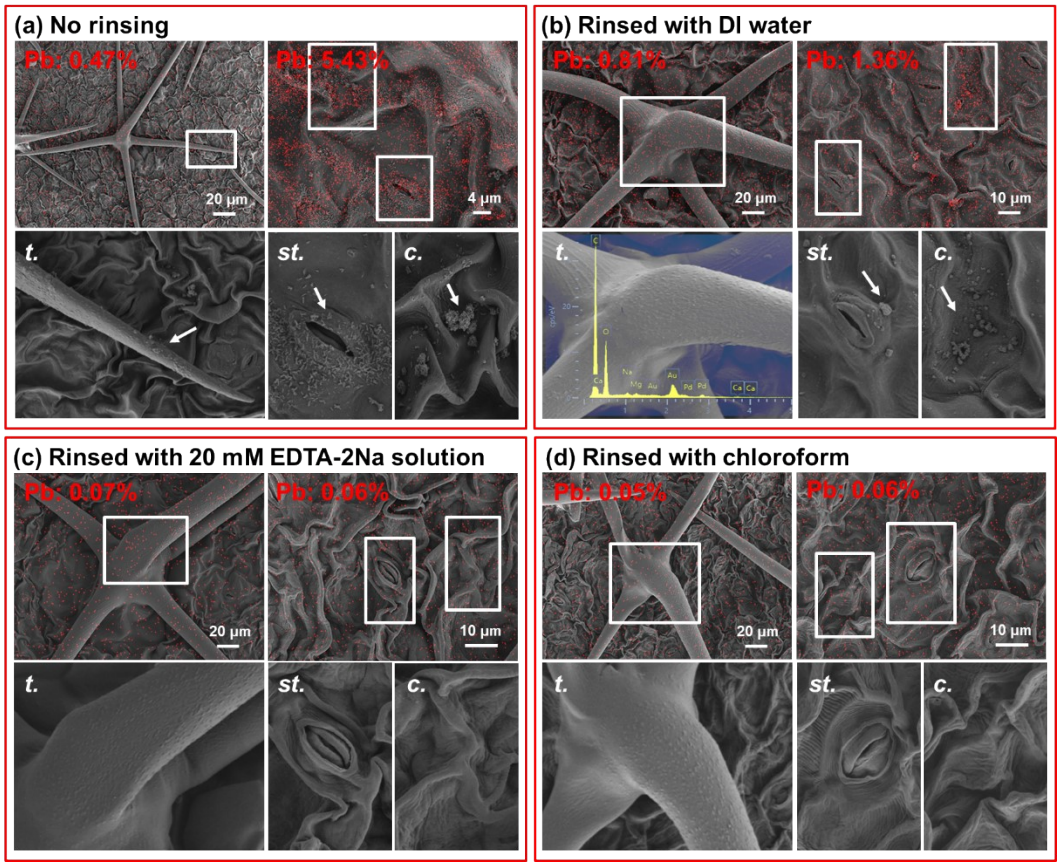

Fig. S19 SEM-EDS images of eggplant leaves after exposure to PbO_2 (M_{Pb} = 170 μg) for 5 days. (a) No rinsing; (b) Rinsed with deionized water; (c) Rinsed with 20 mM EDTA-2Na solution; (d) Rinsed with chloroform. Red dots represent element Pb. Red numbers in upper panels are percentage of element Pb by weight. White arrows indicate large aggregates of PbX_n. Enlarged pictures of leaf structures in white boxes are shown in lower panels. *t.*: *trichome*; *st.*: *stoma*; *c.*: *cuticle*.

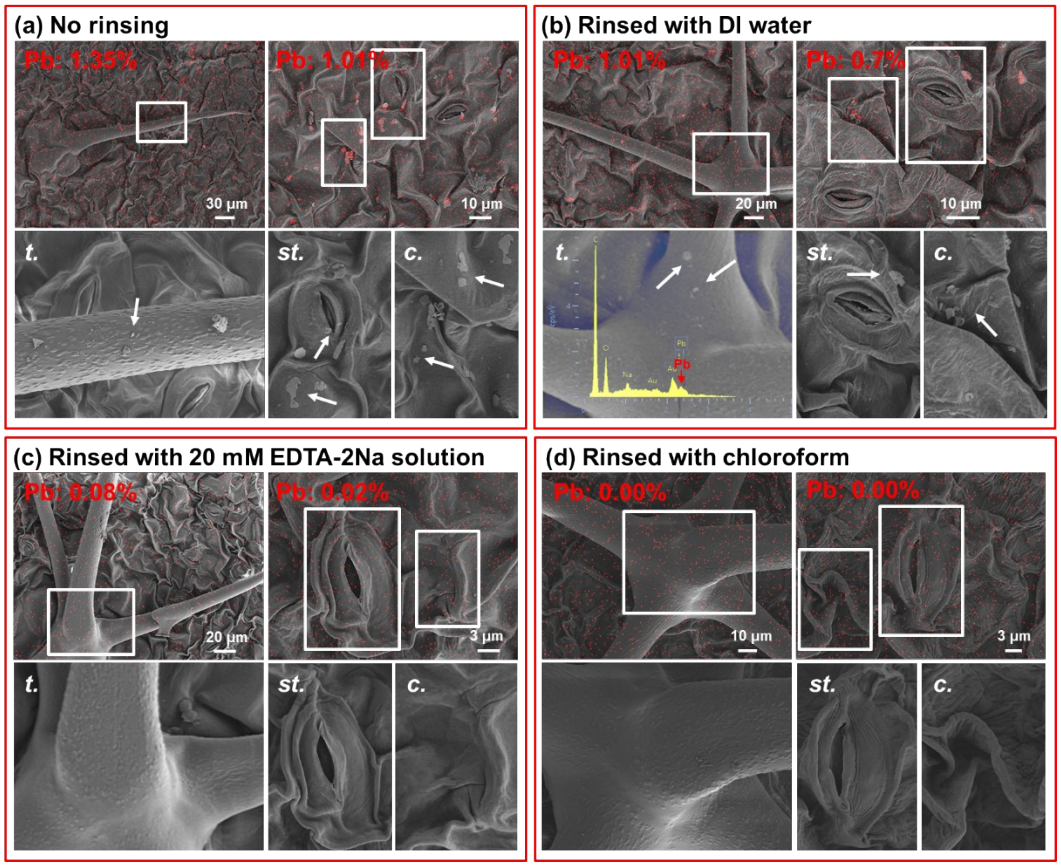

Fig. S20 SEM-EDS images of eggplant leaves after exposure to PbO (M_{Pb} = 170 μg) for 5 days. (a) No rinsing; (b) Rinsed with deionized water; (c) Rinsed with 20 mM EDTA-2Na solution; (d) Rinsed with chloroform. Red dots represent element Pb. Red numbers in upper panels are percentage of element Pb by weight. White arrows indicate large aggregates of PbX_n. Enlarged pictures of leaf structures in white boxes are shown in lower panels. *t.*: *trichome*; *st.*: *stoma*; *c.*: *cuticle*.

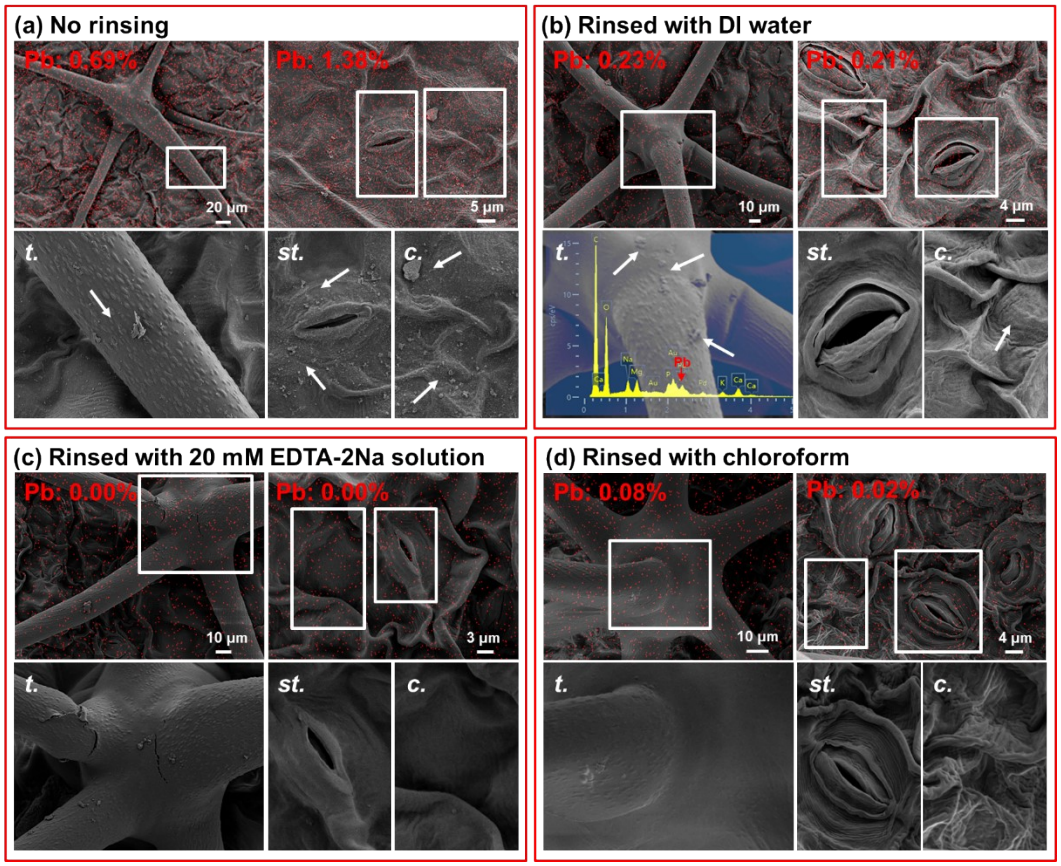

Fig. S21 SEM-EDS images of eggplant leaves after exposure to $PbSO_4$ (M_{Pb} = 170 μg) for 5 days. (a) No rinsing; (b) Rinsed with deionized water; (c) Rinsed with 20 mM EDTA-2Na solution; (d) Rinsed with chloroform. Red dots represent element Pb. Red numbers in upper panels are percentage of element Pb by weight. White arrows indicate large aggregates of PbX_n. Enlarged pictures of leaf structures in white boxes are shown in lower panels. *t.*: *trichome*; *st.*: *stoma*; *c.*: *cuticle*.

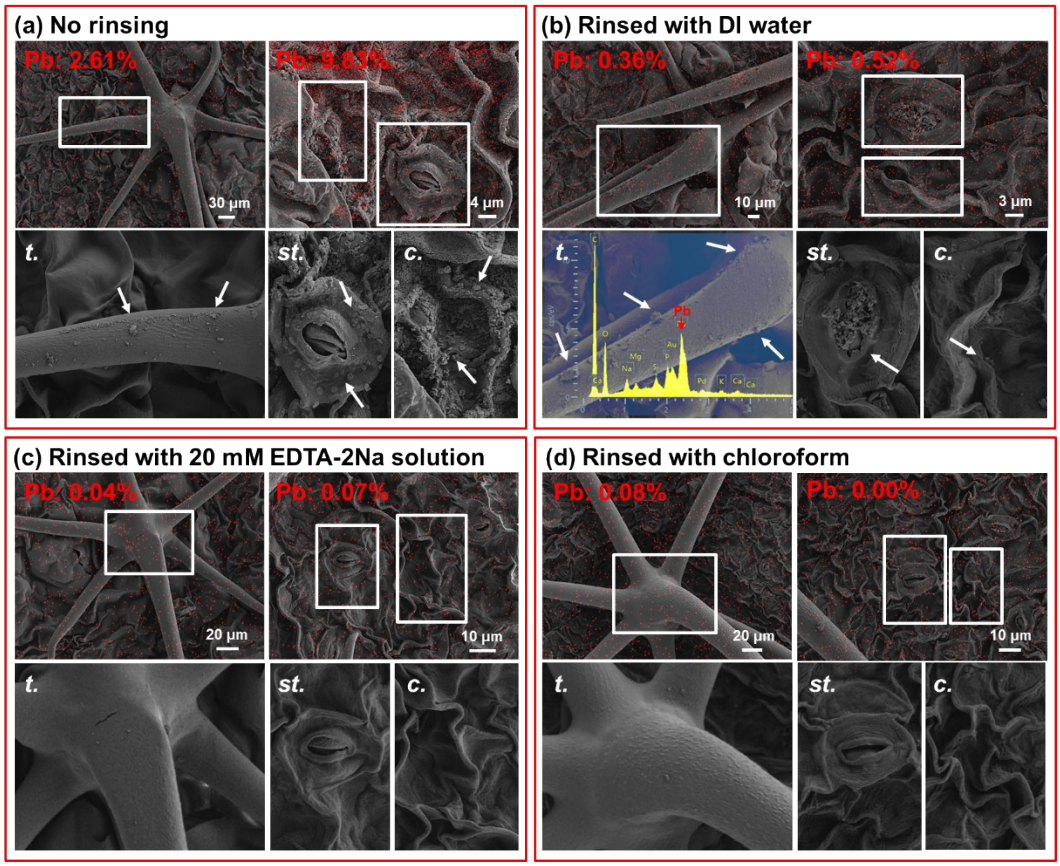

Fig. S22 SEM-EDS images of eggplant leaves after exposure to $PbCl_2$ (M_{Pb} = 170 μg) for 5 days. (a) No rinsing; (b) Rinsed with deionized water; (c) Rinsed with 20 mM EDTA-2Na solution; (d) Rinsed with chloroform. Red dots represent element Pb. Red numbers in upper panels are percentage of element Pb by weight. White arrows indicate large aggregates of PbX_n. Enlarged pictures of leaf structures in white boxes are shown in lower panels. *t.*: *trichome*; *st.*: *stoma*; *c.*: *cuticle*.

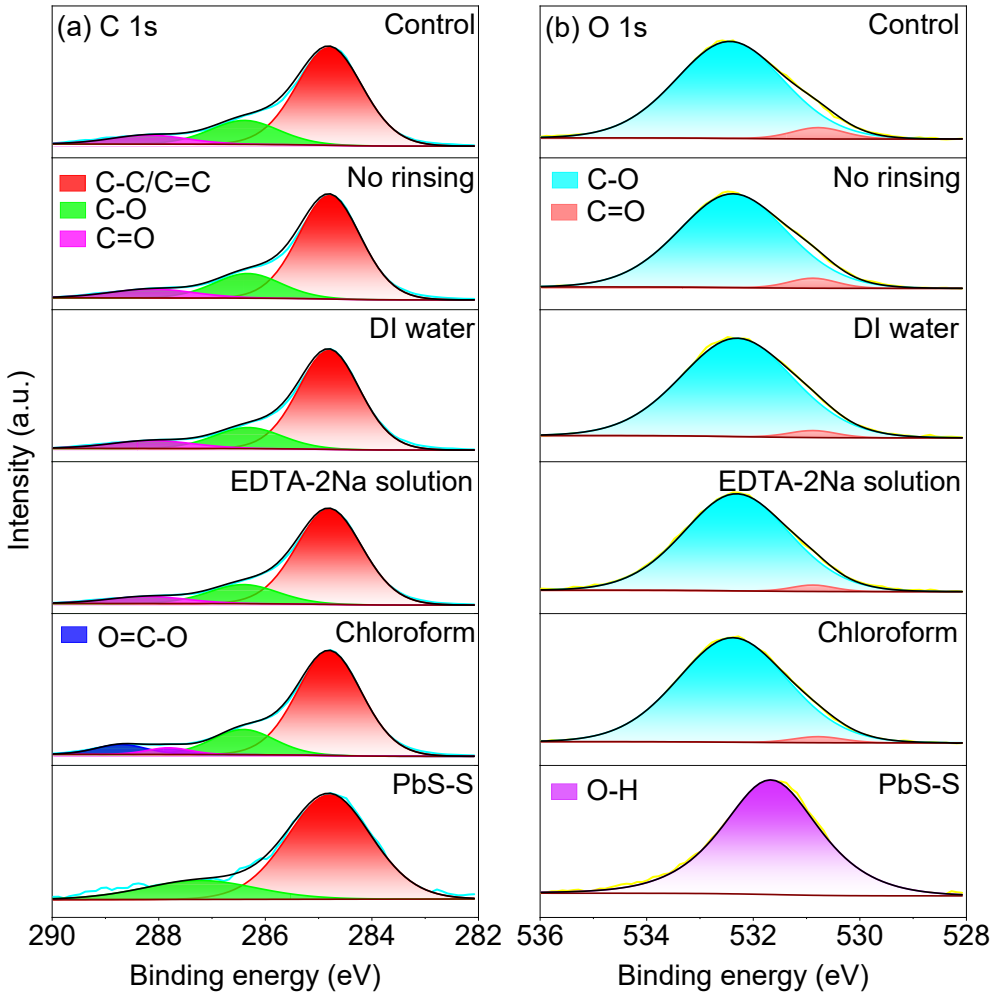

Fig. S23 XPS spectra of different rinsing methods after PbS-S leaf exposure. (a) Fitting results of C 1s spectra; (b) Fitting results of O 1s spectra.

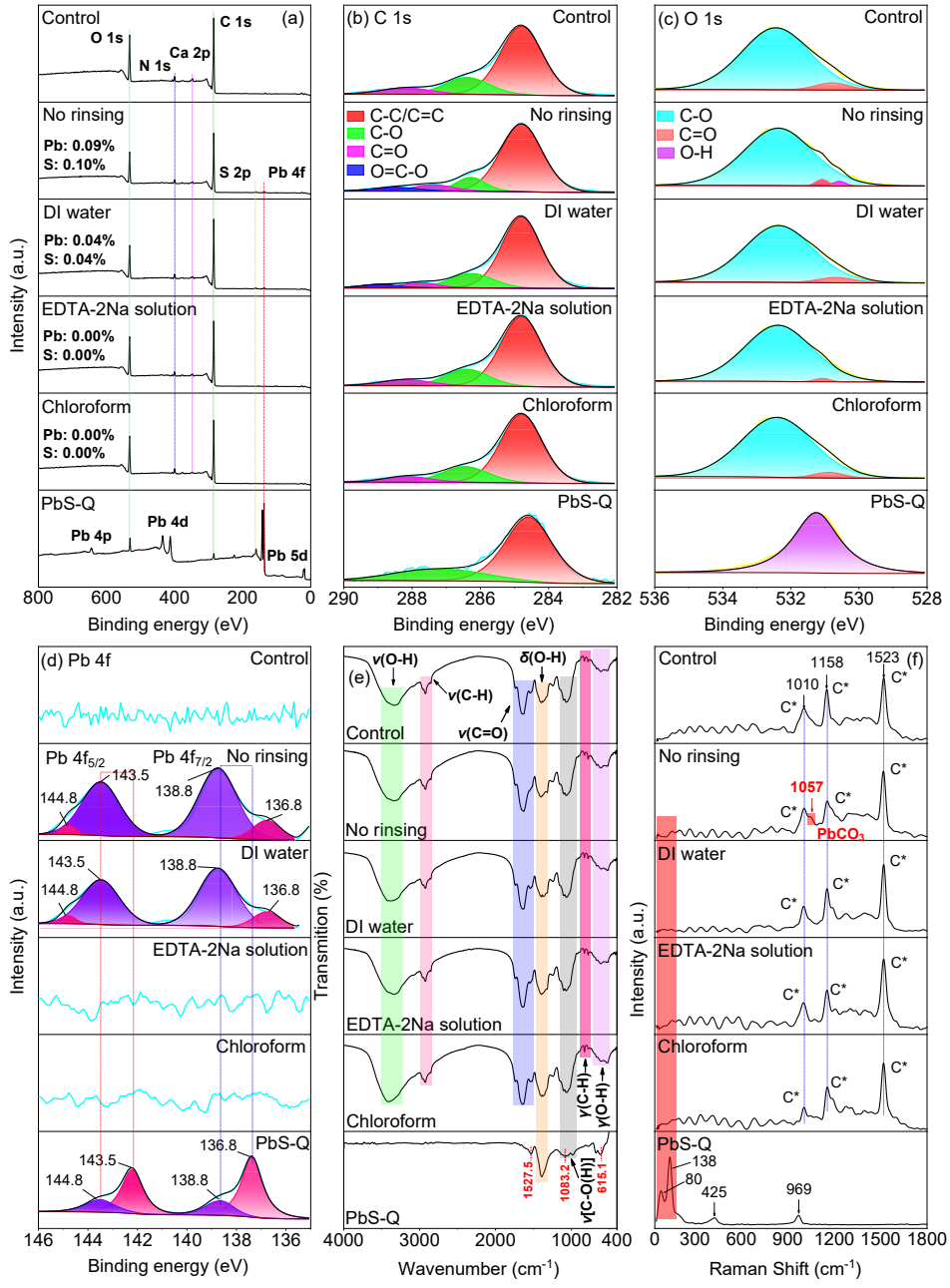

Fig. S24 Characterization images of eggplant leaves after exposure to PbS-Q (M_{Pb} = 170 μg) for 5 days. (a) XPS survey spectra; (b) Fitting results of C 1s spectra; (c) Fitting results of O 1s spectra; (d) Fitting results of Pb 4f spectra; (e) FT-IR spectra. ν: stretching vibration bands. δ: in-plane bending vibration bands. γ: out-of-plane bending vibration bands; (f) Raman spectra. C* is related to Carbon species.

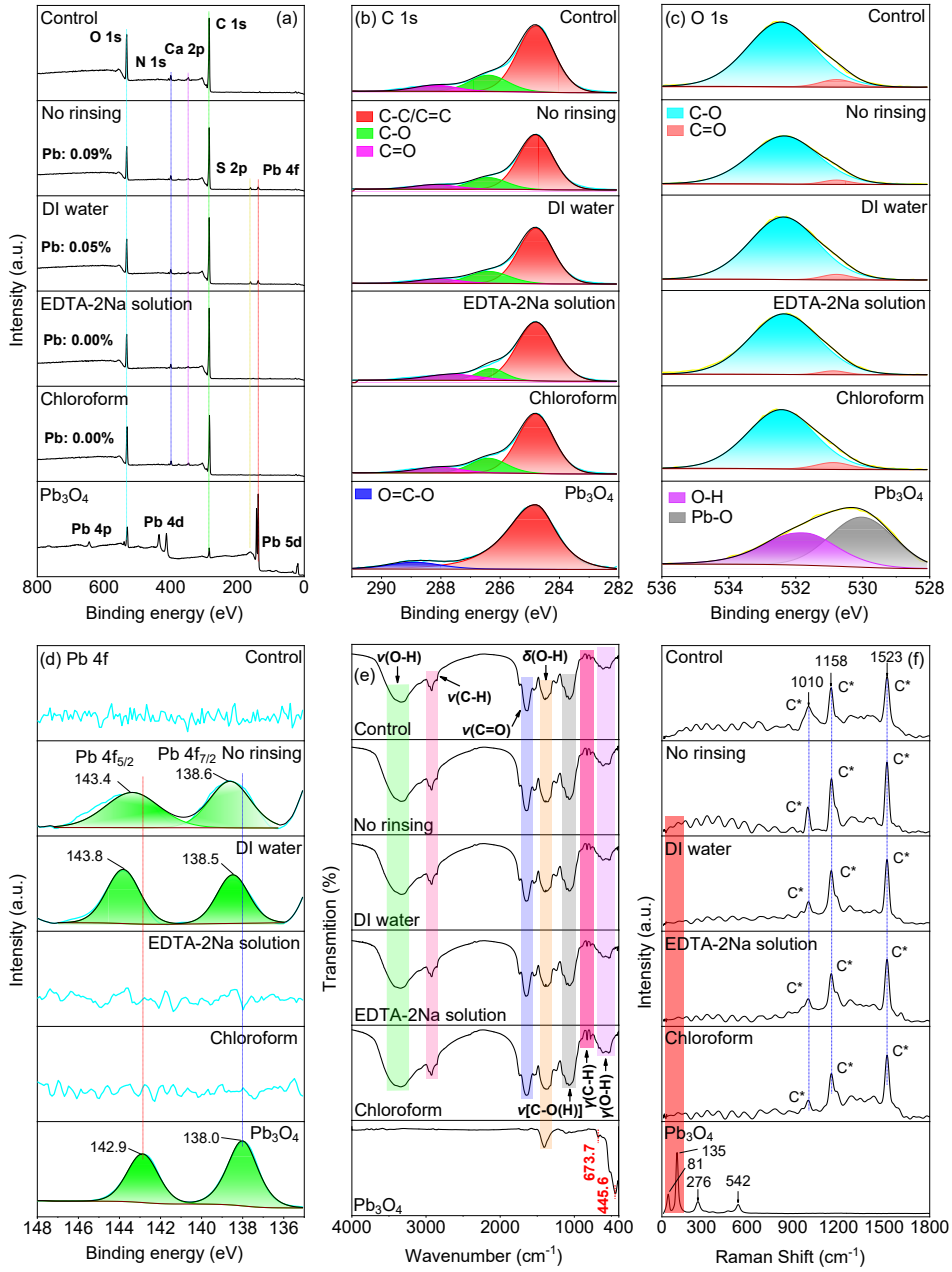

Fig. S25 Characterization images of eggplant leaves after exposure to Pb_3O_4 (M_{Pb} = 170 μg) for 5 days. (a) XPS survey spectra; (b) Fitting results of C 1s spectra; (c) Fitting results of O 1s spectra; (d) Fitting results of Pb 4f spectra; (e) FT-IR spectra. ν: stretching vibration bands. δ: in-plane bending vibration bands. γ: out-of-plane bending vibration bands; (f) Raman spectra. C* is related to Carbon species.

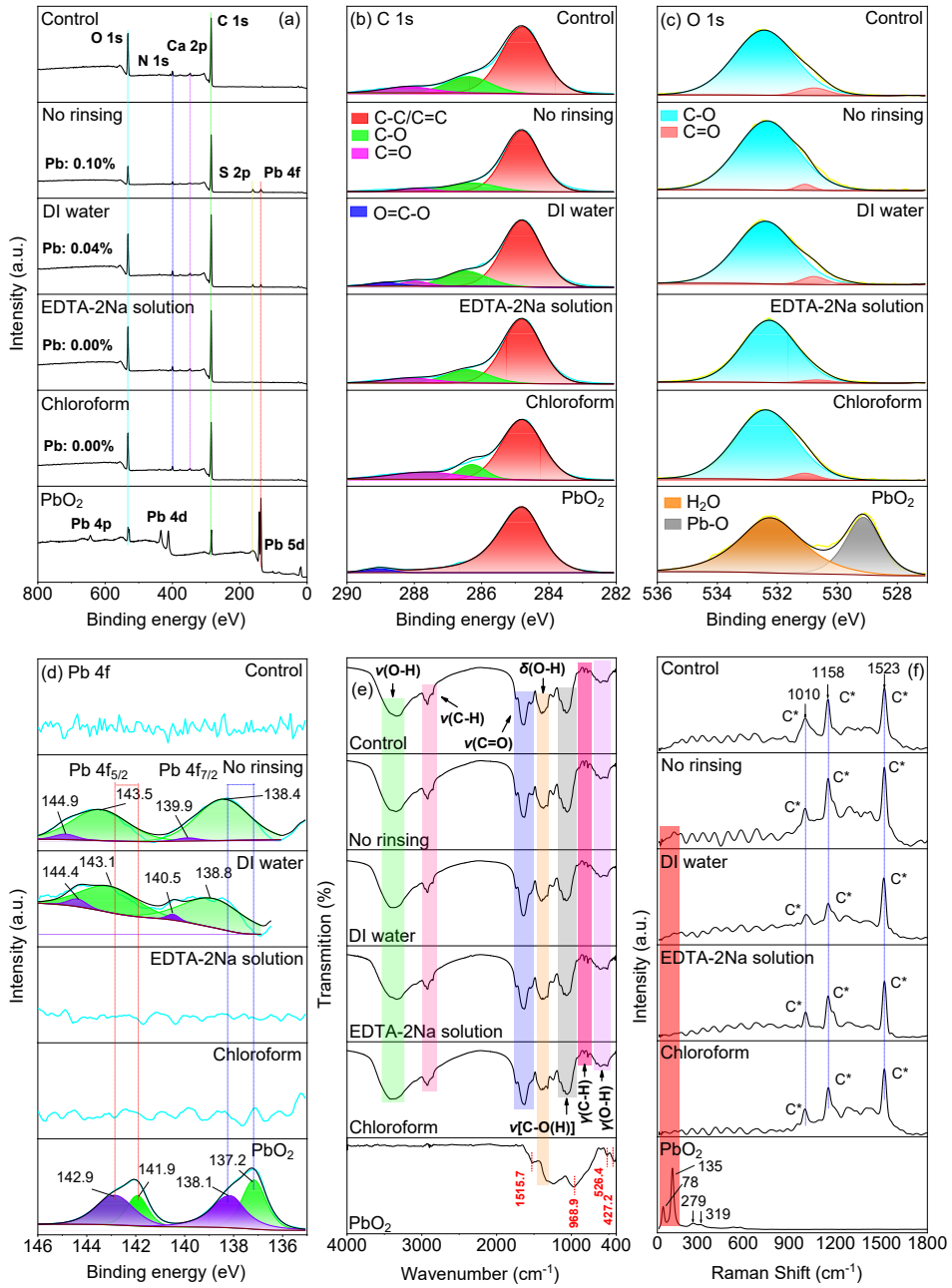

Fig. S26 Characterization images of eggplant leaves after exposure to PbO_2 (M_{Pb} = 170 μg) for 5 days. (a) XPS survey spectra; (b) Fitting results of C 1s spectra; (c) Fitting results of O 1s spectra; (d) Fitting results of Pb 4f spectra; (e) FT-IR spectra. *ν*: stretching vibration bands. *δ*: in-plane bending vibration bands. *γ*: out-of-plane bending vibration bands; (f) Raman spectra. C* is related to Carbon species.

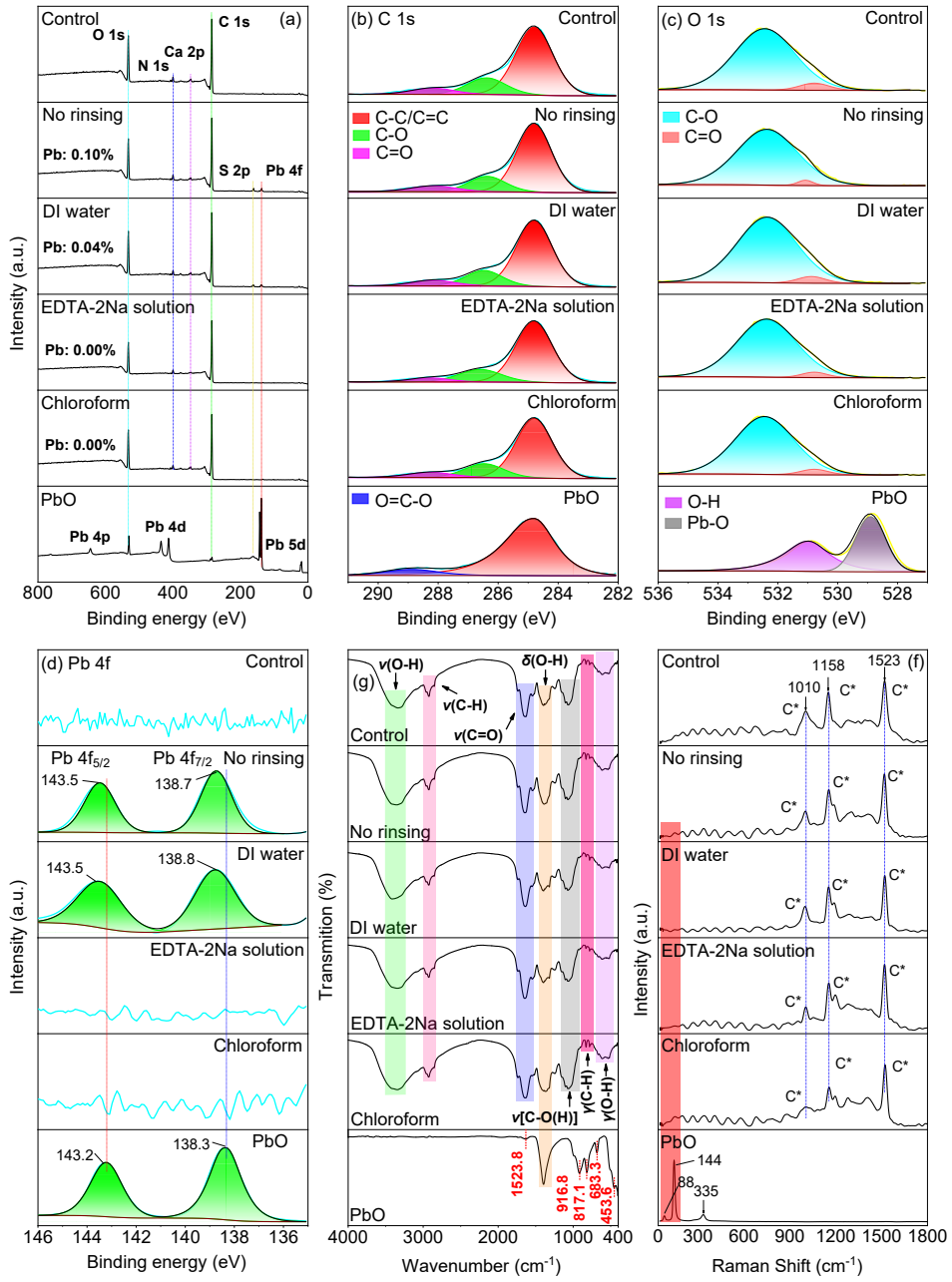

Fig. S27 Characterization images of eggplant leaves after exposure to PbO (M_{Pb} = 170 μg) for 5 days. (a) XPS survey spectra; (b) Fitting results of C 1s spectra; (c) Fitting results of O 1s spectra; (d) Fitting results of Pb 4f spectra; (e) FT-IR spectra. *ν*: stretching vibration bands. *δ*: in-plane bending vibration bands. *γ*: out-of-plane bending vibration bands; (f) Raman spectra. C* is related to Carbon species.

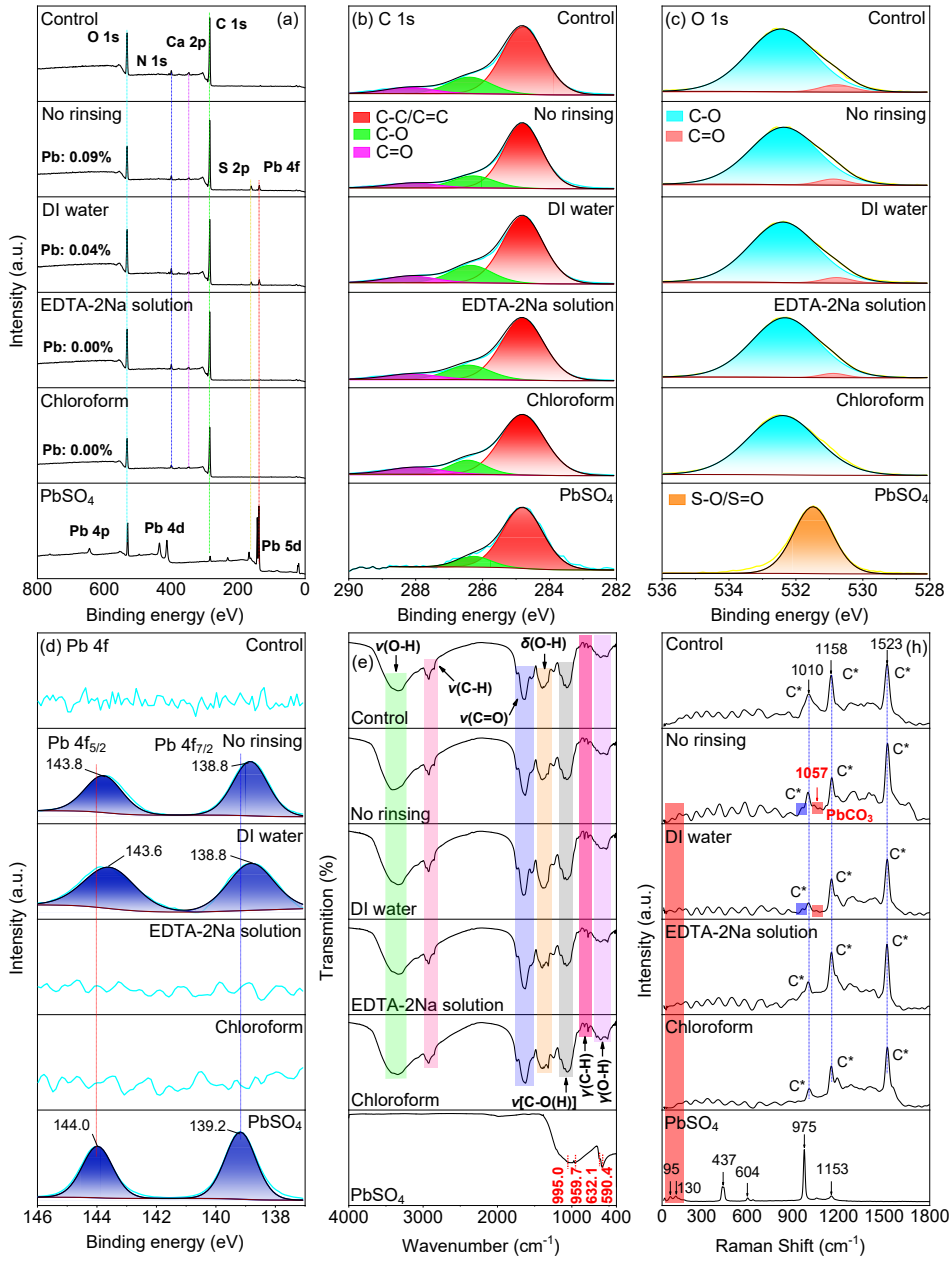

Fig. S28 Characterization images of eggplant leaves after exposure to $PbSO_4$ (M_{Pb} = 170 μg) for 5 days. (a) XPS survey spectra; (b) Fitting results of C 1s spectra; (c) Fitting results of O 1s spectra; (d) Fitting results of Pb 4f spectra; (e) FT-IR spectra. *ν*: stretching vibration bands. *δ*: in-plane bending vibration bands. *γ*: out-of-plane bending vibration bands; (f) Raman spectra. C* is related to Carbon species.

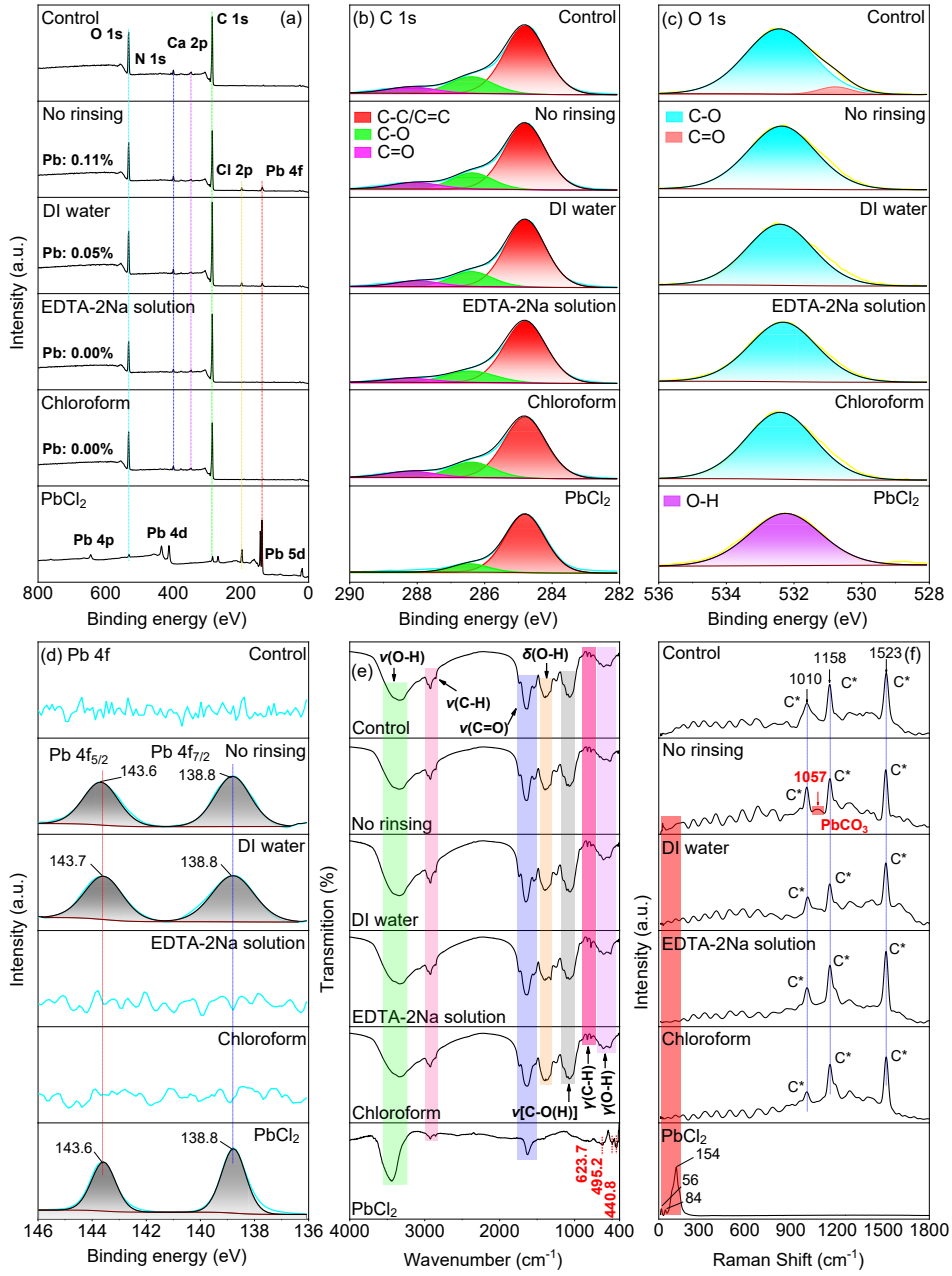

Fig. S29 Characterization images of eggplant leaves after exposure to $PbCl_2$ (M_{Pb} = 170 μg) for 5 days. (a) XPS survey spectra; (b) Fitting results of C 1s spectra; (c) Fitting results of O 1s spectra; (d) Fitting results of Pb 4f spectra; (e) FT-IR spectra. *ν*: stretching vibration bands. *δ*: in-plane bending vibration bands. *γ*: out-of-plane bending vibration bands; (f) Raman spectra. C* is related to Carbon species.

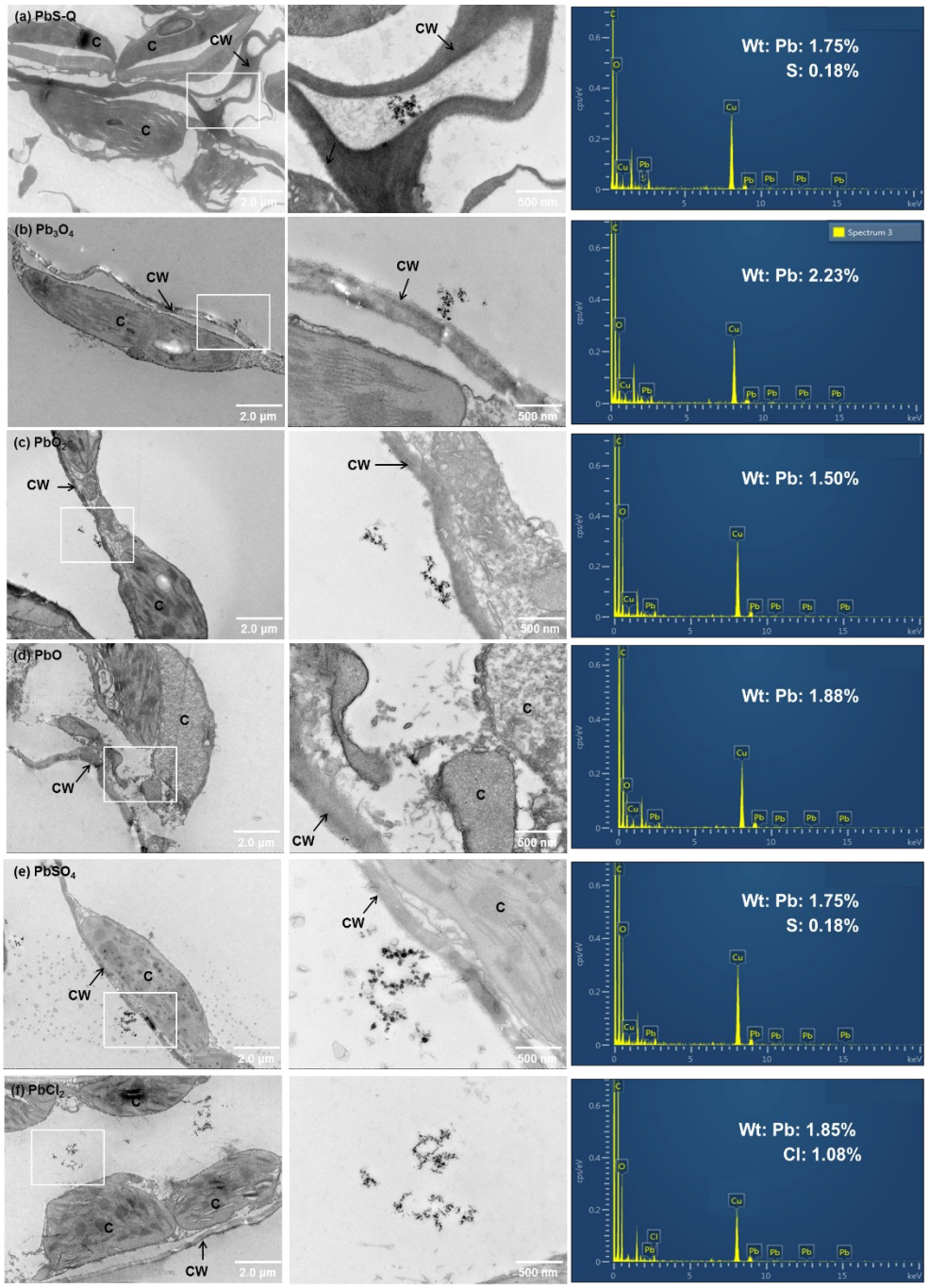

Fig. S30 Transmission electron microscopy energy-dispersive spectroscopy (TEM-EDS) analysis of Pb-rich regions on eggplant leaves exposed to PbX_n for 5 days. Wt: weight percentage. CW: cell wall; C: chloroplast.

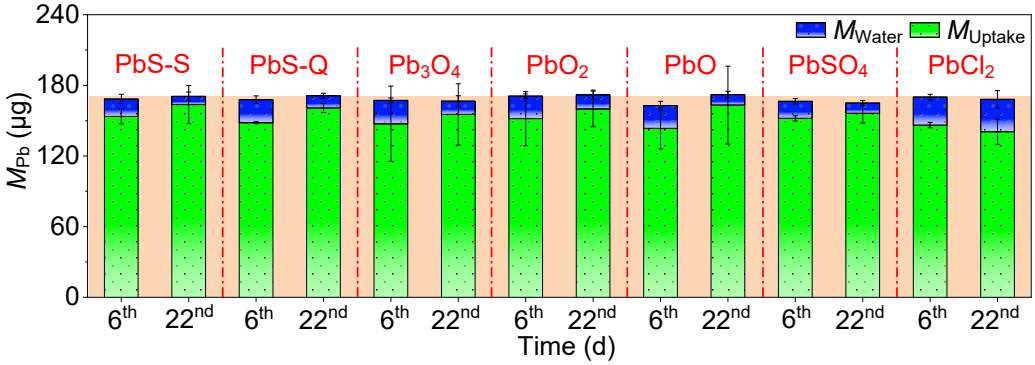

Fig. S31 Mass of lead (M_{Pb}) in eggplant leaves (M_{Uptake}) or deionized water (M_{Water}). Total amount of Pb applied to leaves at each experiment period is indicate by the pink background. Data are mean ± SD (n = 5).

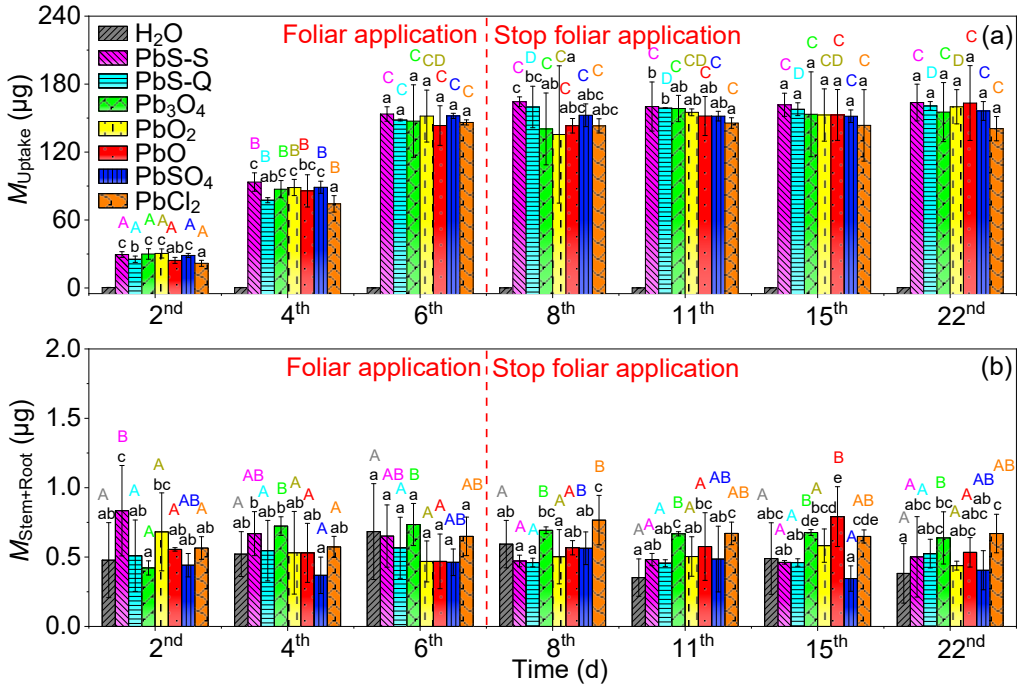

Fig. S32 Significant testing of mass or concentration of Pb in different organs of eggplant. (a) Total amount of Pb in leaves after rinsing with deionized water, $M_{Adhesion}$. The capital letters on

top of columns indicate significant differences between different exposure days for each Pb species ($p < 0.05$). The lowercase letters on top of columns indicate significant differences between different Pb species on the same day ($p < 0.05$); (b) Mass of Pb in stems and roots ($M_{Stem+Root}$). The capital letters on top of columns indicate significant differences between different exposure days for each Pb species ($p < 0.05$). The lowercase letters on top of columns indicate significant differences between different Pb species on the same day ($p < 0.05$). Data are mean ± SD (n = 5).

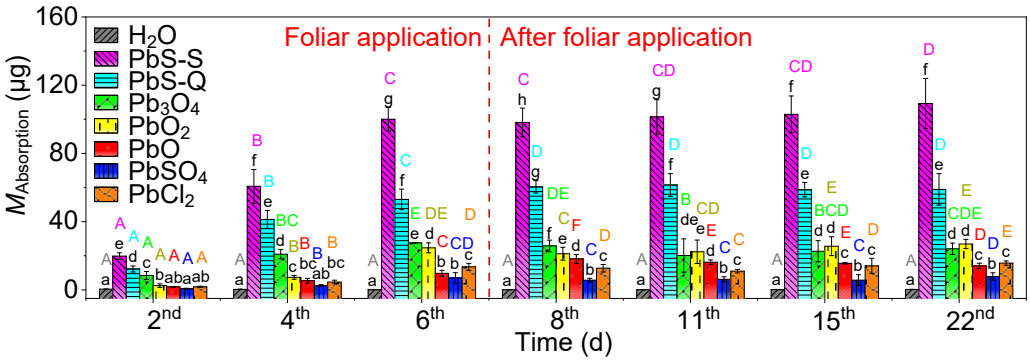

Fig. S33 Significant testing of uptake mass of Pb in leaves after rinsing with 20 mM EDTA-2Na solution. The capital letters on top of columns indicate significant differences between different exposure days for each Pb species ($p < 0.05$). The lowercase letters on top of columns indicate significant differences between different Pb species on the same day ($p < 0.05$). Data are mean ± SD (n = 5).

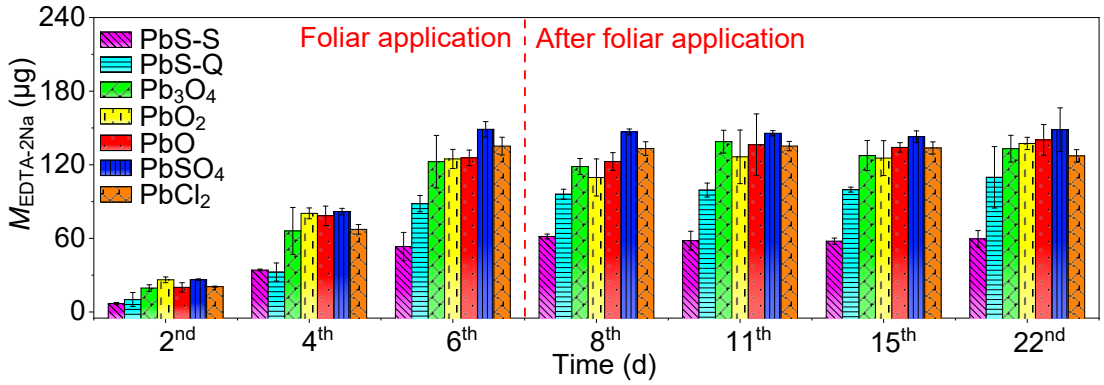

Fig. S34 Mass of Pb in 20 mM EDTA-2Na solution, $M_{EDTA-2Na}$. Data are mean ± SD (n = 5).

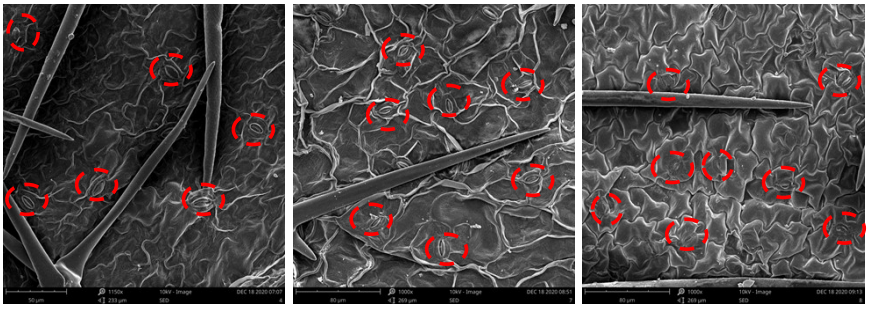

Fig. S35 Closed stomata of eggplant leaves surface on the 2nd, 4th and 6th days after 1 mM abscisic acid (ABA) treatment.

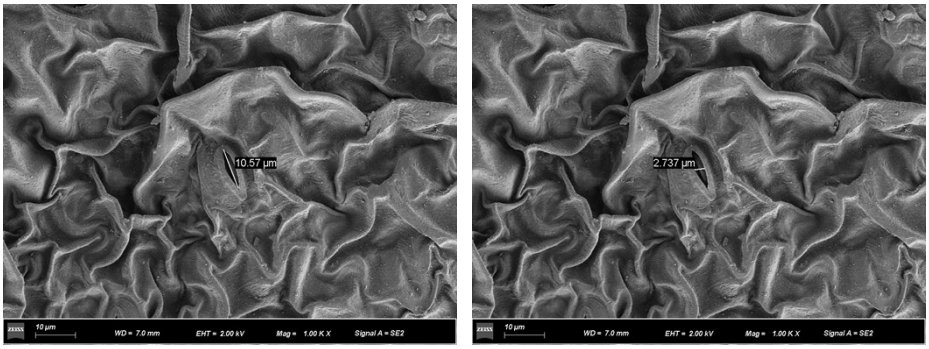

Fig. S36 Sizes of stomata on eggplant leaves.

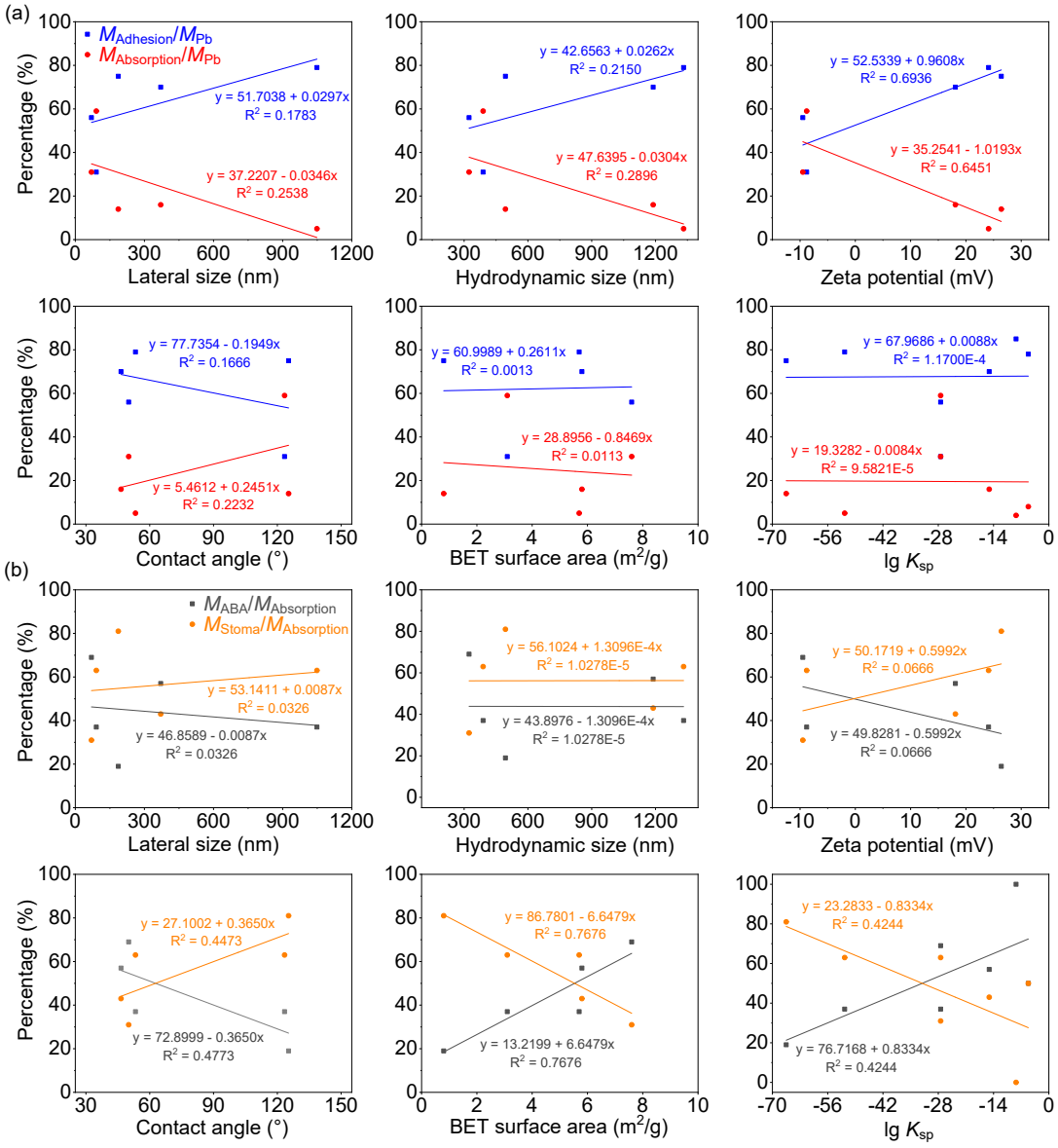

Fig. S37 Variations of (a) adhesion/absorption rates ($M_{Adhesion}/M_{Pb}$ or $M_{Absorption}/M_{Pb}$) (M_{Pb} = 170 μg) or (b) wax/stomatal absorption rates ($M_{ABA}/M_{Absorption}$ or $M_{Stoma}/M_{Absorption}$) of Pb species with single surface property.

References

1. G. J. Zhou, M. K. Lü, Z. L. Xiu, S. F. Wang, H. P. Zhang, Y. Y. Zhou and S. M. Wang, Controlled synthesis of high-quality PbS star-shaped dendrites, multipods, truncated nanocubes, and nanocubes and their shape evolution process, *J. Phys. Chem. B*, 2006, **110**, 6543-6548.
2. Q. L. Yu, M. Q. Sun, Y. Wang, M. C. Li and L. Liu, The interaction between lead sulfide nano-dendrites and Saccharomyce cerevisiae is involved in nanotoxicity, *RSC Adv.*, 2014, **4**, 20371-20378.
3. K. Park, S. Park, J. Choi, G. Kim, M. Tong and H. Kim, Influence of excess sulfide ions on the malachite-bubble interaction in the presence of thiol-collector, *Sep. Purif. Technol.*, 2016, **168**, 1-7.
4. Y. L. Zhao, S. C. Kang, L. Qin, W. N. Wang, T. T. Zhang, S. X. Song and S. Komarneni, Self-assembled gels of Fe-chitosan/montmorillonite nanosheets: Dye degradation by the synergistic effect of adsorption and photo-Fenton reaction, *Chem. Eng. J.*, 2020, **379**.
5. W. J. Peng, G. H. Han, Y. J. Cao, K. G. Sun and S. X. Song, Efficiently removing Pb(II) from wastewater by graphene oxide using foam flotation, *Colloid. Surface. A*, 2018, **556**, 266-272.
6. I. V. Filippova, L. O. Filippov, Z. Lafhaj, O. Barres and D. Fornasiero, Effect of calcium minerals reactivity on fatty acids adsorption and flotation, *Colloid. Surface. A*, 2018, **545**, 157-166.
7. Q. C. Feng, S. M. Wen, W. J. Zhao, J. S. Deng and Y. J. Xian, Adsorption of sulfide ions on cerussite surfaces and implications for flotation, *Appl.Surf. Sci.*, 2016, **360**, 365-372.
8. L. Y. Dong, F. Jiao, W. Q. Qin, H. L. Zhu and W. H. Jia, Activation effect of lead ions on scheelite flotation: Adsorption mechanism, AFM imaging and adsorption model, *Sep. Purif. Technol.*, 2019, **209**, 955-963.
9. A. V. Shchukarev and D. V. Korolkov, XPS study of group IA carbonates, *Cent. Eur. J. Chem.*, 2004, **2**, 347-362.
10. S. Rondon and P. M. A. Sherwood, Core Level and Valence Band Spectra of PbO by XPS, *Surf. Sci. Spectra*, 1998, **5**, 97-103.
11. R. T. Guo, C. Z. Lu, W. G. Pan, W. L. Zhen, Q. S. Wang, Q. L. Chen, H. L. Ding and N. Z. Yang, A comparative study of the poisoning effect of Zn and Pb on Ce/TiO2 catalyst for low temperature selective catalytic reduction of NO with NH3, *Catal. Commun.*, 2015, **59**, 136-139.
12. Z. H. Lian, F. D. Liu, H. He, X. Y. Shi, J. S. Mo and Z. B. Wu, Manganese–niobium mixed oxide catalyst for the selective catalytic reduction of NOx with NH3 at low temperatures, *Chem. Eng. J.*, 2014, **250**, 390-398.
13. H. Lai, J. S. Deng, S. M. Wen and Q. J. Liu, Elucidation of lead ions adsorption mechanism on marmatite surface by PCA-assisted ToF-SIMS, XPS and zeta potential, *Miner. Eng.*, 2019, **144**, 106035.
14. M. A. Hampton, C. Plackowski and A. V. Nguyen, Physical and chemical analysis of elemental sulfur formation during galena surface oxidation, *Langmuir*, 2011, **27**, 4190-4201.
15. Y. L. Mikhlin, A. A. Karacharov and M. N. Likhatski, Effect of adsorption of butyl xanthate on galena, PbS, and HOPG surfaces as studied by atomic force microscopy and spectroscopy and XPS, *Internat. J. Miner. Process.*, 2015, **144**, 81-89.
16. J. T. Bi, X. Huang, J. K. Wang, T. Wang, H. Wu, J. Y. Yang, H. J. Lu and H. X. Hao, Oil-phase cyclic magnetic adsorption to synthesize Fe3O4@C@TiO2-nanotube composites for

simultaneous removal of Pb(II) and Rhodamine B, *Chem. Eng. J.*, 2019, **366**, 50-61.
17. J. Liu, M. Ejtemaei, A. V. Nguyen, S. M. Wen and Y. Zeng, Surface chemistry of Pb-activated sphalerite, *Miner. Eng.*, 2020, **145**.
18. Z. Lv, Z. Chen, Q. Yu, W. Zhu, H. You, B. Chen, Z. Zheng, Y. Liu and Q. Hu, Micro-area investigation on electrochemical performance improvement with Co and Mn doping in PbO2 electrode materials, *RSC Adv.*, 2021, **11**, 28949-28960.
19. L. R. Pederson, Two-dimensional chemical-state plot for lead using XPS, *J. Electron Spectrosc.*, 1982, **28**, 203-209.
20. P. U, A. Gowda K M, E. M G, S. T B, N. N and R. M B, Biologically synthesized PbS nanoparticles for the detection of arsenic in water, *Int. Biodeter. Biodegr.*, 2017, **119**, 78-86.
21. M. Suganya, S. Anitha, D. Prabha, S. Balamurugan, J. Srivind and A. R. Balu, Enhanced photocatalytic and antifungal properties of Sr-doped PbS nanopowders, *Mater. Technol.*, 2017, **33**, 214-219.
22. Y. R. Zhao, J. L. Wang, A. Z. Pan, L. He and S. Simon, Degradation of red lead pigment in the oil painting during UV aging, *Color Res. Appl.*, 2019, **44**, 790-797.
23. D. Sister and E. Minopoulou, A study of smalt and red lead discolouration in Antiphonitis wall paintings in Cyprus, *Appl. Phys. A-Mater.*, 2009, **96**, 701-711.
24. F. H. ElBatal, M. A. Marzouk, H. A. ElBatal and F. M. EzzElDin, Impact effect of gamma irradiation on the optical, FTIR, ESR spectral properties and thermal behavior of some mixed (PbO + Bi2O3) borate glasses searching for shielding effects, *J. Mol. Struct.*, 2022, **1267**.
25. J. J. Boon, F. Hoogland, K. Keune and H. M. Parkin, in *AIC Paintings Specialty Group Postprints*, 2006, vol. 19, pp. 16-23.
26. L. H. Xu, J. Tian, H. Q. Wu, Z. Y. Lu, Y. H. Yang, W. Sun and Y. H. Hu, Effect of Pb 2+ ions on ilmenite flotation and adsorption of benzohydroxamic acid as a collector, *Appl. Surf. Sci.*, 2017, **425**, 796-802.
27. D. H. Lee and S. Condrate, FTIR spectral characterization of thin film coatings of oleic acid on glasses: I. Coatings on glasses from ethyl alcohol, *J. Mater. Sci.*, 1999, **34**, 139-146.
28. C. Liné, J. Reyes-Herrera, M. Bakshi, M. Wazne, V. Costa, D. Roujol, E. Jamet, H. Castillo-Michel, E. Flahaut and C. Larue, Fourier transform infrared spectroscopy contribution to disentangle nanomaterial (DWCNT, TiO2) impacts on tomato plants, *Environ. Sci.-Nano*, 2021, **8**, 2920-2931.
29. S. V. Ovsyannikov, V. V. Shchennikov, A. Cantarero, A. Cros and A. N. Titov, Raman spectra of (PbS)1.18(TiS2)2 misfit compound, *Mat. Sci. Eng. A-Struct.*, 2007, **462**, 422-426.
30. M. S. Pawar, P. K. Bankar, M. A. More and D. J. Late, PbS Nanostar-Like Structures as Field Emitters, *ChemistrySelect*, 2017, **2**, 5175-5179.
31. G. D. Smith, S. Firth, R. J. H. Clark and M. Cardona, First- and second-order Raman spectra of galena (PbS), *J. Appl. Phys.*, 2002, **92**, 4375-4380.
32. J. P. Ge, J. Wang, H. X. Zhang, X. Wang, Q. Peng and Y. D. Li, Orthogonal PbS nanowire arrays and networks and their Raman scattering behavior, *Chem.-Eur. J.*, 2005, **11**, 1889-1894.
33. D. P. Guo, C. Robinson and J. E. Herrera, Mechanism of dissolution of minium (Pb3O4) in water under depleting chlorine conditions, *Corros. Sci.*, 2016, **103**, 42-49.
34. G. Trettenhahn, G. Nauer and A. Neckel, Vibrational spectroscopy on the PbO-PbSO4 system and some related compounds: part 1. Fundamentals, infrared and Raman spectroscopy, *Vib. spectrosc.*, 1993, **5**, 85-100.
35. H. G. Edwards, D. W. Farwell, E. M. Newton and F. R. Perez, Minium; FT-Raman non-destructive analysis applied to an historical controversy, *Analyst*, 1999, **124**, 1323-1326.

36. L. Burgio, R. J. Clark and S. Firth, Raman spectroscopy as a means for the identification of plattnerite (PbO2), of lead pigments and of their degradation products, *Analyst*, 2001, **126**, 222-227.